OPTIMIZATION STUDY OF DIISOPROPANOLAMINE (DIPA) DEGRADATION USING PHOTO-FENTON PROCESS SCOPE: VISIBLE LIGHT

By

YEN KA WAI

13886

A project dissertation submitted in partial fulfilment of
the requirements for the
Bachelor of Engineering (Hons)
(Chemical Engineering)

May 2014

Universiti Teknologi PETRONAS
Bandar Seri Iskandar
31750 Tronoh
Perak Darul Ridzuan

CERTIFICATION OF APPROVAL

Optimization Study of Diisopropanolamine (DIPA) Degradation using Photo-Fenton Process Scope: Visible Light

By
Yen Ka Wai
13886

A project dissertation submitted to
Chemical Engineering Programme
Universiti Teknologi PETRONAS
in partial fulfilment of the requirement for the
BACHELOR OF ENGINEERING (Hons)
(CHEMICAL)

Approved by,

_____
(Assoc. Prof. Dr. Mohd. Azmi B Bustam @ Khalil)

UNIVERSITI TEKNOLOGI PETRONAS
TRONOH, PERAK
MAY 2014

CERTIFICATION OF ORIGINALITY

This is to certify that I am responsible for the work submitted in this project, that the original work is my own except as specified in the references and acknowledgements, and that the original work contained herein have not been undertaken or done by unspecified sources or persons.

_____

(YEN KA WAI)

ABSTRACT

Advanced Oxidation Process (AOP) is regarded as one of the chemical treatment specifically designed to remove contaminants and unwanted compositions in the form of organic or inorganic matters. The technology is founded on the complex oxidation reaction utilizing hydroxyl radicals to breakdown waste. Under universal assessment, well-known electricity generation fossil fuel plant via raw natural gas produces heavy gaseous hydrocarbons, acid gases, water and liquid hydrocarbons. Thus, typical gas treating mechanism using amine solvents is required to remove the corrosive and toxicity properties within the existence of carbon dioxide and hydrogen sulphide in natural gas. AOPs treatment is later necessitated for the subsequent amine solvent mechanism. The research project will focus on the Photo-Fenton process, one of AOP's most effective treatment, and the optimized parameters affecting the degradation standard of Diisopropanolamine (DIPA). The amine waste used will be DIPA and the seven parameters being studied covers the concentration of hydrogen peroxide solution, intensity of light, temperature, concentration of DIPA, concentration of ferrous sulphate heptahydrate, reaction time and pH value. Moreover, the experimental work will study the Chemical Oxygen Demand (COD) by utilizing the Hach DRB 200 Digester and Hach® DR3900 Spectrophotometer. Initial experimental setup is calibrated with blank DIPA concentration measurement of 1302mg/L. In design of experimentation, the maximum optimization value is achieved by sample run 14 which is 662mg/L COD removal (50.84% removal) while the lowest value is achieved by sample run 3 which is 32mg/L COD removal (2.46% removal). Results for factorial experimental design is arranged with the highest order of significance towards lowest order of significance; concentration of H_2O_2 which is followed closely with concentration of $FeSO_4.7H_2O$ towards temperature and lastly, light intensity. Later onwards, optimization process adjusted at 1.0M concentration of H_2O_2, 0.5M concentration of $FeSO_4.7H_2O$, temperature of 35^oC and light intensity of 300Watt; achieved COD measurement of 531mg/L (771mg/L removal, 59.22% removal). Comparison for significance of temperature and light intensity indicated their absence of varying reaction kinetics which produced lower COD removal rate of 22.81% (1005mg/L COD measurement).

ACKNOWLEDGEMENT

Through this acknowledgement, I would like to express my greatest amplitude to the people who have helped and supported me throughout the project period. First and foremost, the compliments should be given towards the Chemical Engineering department of Universiti Teknologi PETRONAS (UTP) and the coordinators of the Final Year Project (FYP) course. The countless amounts of necessary arrangements, briefings, seminars and workshops are provided in an organized manner.

The success and final outcome of the specific project was mainly preceded by my supervisor, Associate Professor Dr. Mohd. Azmi B Bustam @ Khalil. The gratitude is highly attributed according to his endless support and guidance. With the regards as the director of CO_2 Capture Research Center, he has many other undertakings and responsibilities. However, he has never failed to spend his precious time to update and to monitor my project.

Besides that, special thanks would be expressed to my co-supervisor, Dr. Nadia Riaz for her kind assistances and patient guidance since the beginning of the research project. Many resourceful knowledge and suggestions are provided during the experimental conduct. The specific information helped a great deal in practical terms for the understanding of the research study.

In addition to that, I would like to extend my gratitude to all the laboratory technicians and colleagues in UTP especially the Chemical Engineering department as well as the CO_2 Capture Research Center personnel. Their assistance and tolerance are highly appreciated especially through the sharing of apparatus and equipment.

All in all, the utmost appreciations should be shared to various individuals who have shared guidance, insights and tolerance either directly or indirectly for the completion of the project.

TABLE OF CONTENTS

LIST OF FIGURES

LIST OF TABLES

ABBREVIATIONS AND NOMENCLATURES

No.	Name	Formula/Short Form
1	Diisopropanolamine	DIPA
2	Hydrogen Peroxide	H_2O_2
3	Ferrous Sulphate Heptahydrate	$FeSO_4.7H_2O$
4	Fenton Reagents	H_2O_2 + $FeSO_4.7H_2O$
5	Hydroxyl Radicals	•OH
6	Sodium Hydroxide	NaOH
7	Sulphuric Acid	H_2SO_4
8	Water	H_2O
9	Advanced Oxidation Process	AOP

1.0 INTRODUCTION

1.1 Background

Special treatments revolving disposure and decomposition are related with the sight of waste products in the natural gas industry, which is one of the major energy resources in the current situation. In the year of 1987, the technology of Advanced Oxidation Process (AOP) has been introduced by Glaze et al. (2003) which utilizes the principle of possible generation of hydroxyl radicals in a sufficient quantity for better purification (Oppenländer, 2003). AOP has been focusing on eliminating amine waste mainly consisting of Monoethanolamine (MEA) and Diethanolamine (DEA). The difference between AOP and conventional oxidation process is the generation of active hydroxyl radical group that will lead to a chain reaction on the oxidation process instead of Redox reaction (reduction-oxidation process) involving loss or gain in valence electrons between two or more elements.

AOPs have always been categorized as a tertiary treatment with the better capability in oxidative degradation process in both organic and inorganic contaminant (Oppenländer, 2003). Application of AOP has been vastly implemented in Europe and in United States which the shifting phase is from company Solar Chem Environmental Systems, Canada towards Chemiviron Carbon, USA. In comparison with the various processes of AOP, Photo-Fenton under visible light is defined as the most efficient towards cost procedure through the comparison table (Y.W. Kang and K.Y. Hwang, 2000). Photo-Fenton process (Fenton reagents, Fe^{2+} and H_2O_2) involves the following stages (Pignatello, 1992; Bossmann et al., 1998); where products of Fenton reagents, Fe(III) complexes react with the Ultra-Violet (UV) energy to produce Fe(II) ions and hydroxyl radical respectively. Later onwards, the photolysis of the Fe(III) complexes will instill regeneration of Fe(II) reagent which further produces hydroxyl radicals as shown in the corresponding formulae:-

$$Fe^{2+} + H_2O_2 \rightarrow Fe^{3+} + OH^- + \bullet OH \qquad \text{(Fenton Reagent)}$$

$$Fe^{3+} + H_2O + hv \rightarrow Fe^{2+} + H^+ + \bullet OH$$

$$Fe(OH)^{2+} + hv \rightarrow Fe^{2+} + \bullet OH$$

According to the Photo-Fenton process, there are many parameters governing the efficiency in terms of photo-degradation standard. On the whole representation, research studies regarding Photo-Fenton under visible light will be significant as to strengthen its assertion as 'the water treatment process of the 21st century' (AES Arabia Ltd., 2013).

1.2 Problem Statement

Advanced Oxidation Process (AOP) is one of the increasingly used processes in recent years for treating water containing toxic organic pollutants (Bolton et al., 2001; Safarzadeh-Amiri et al., 1997; Ghaly et al., 2001; Pera-Titus et al., 2004; Pérez-Moya et al., 2007; Durán et al., 2008). The method covers the types of amine waste only revolving around the likes of Methyldiethanolamine (MDEA) and Monoethanolamine (MEA) respectively through citations such as Sabtanti Harimurti et al., 2011 and Binay K. D. et al., 2010. The idea of investing into another type of secondary alkanolamine, Diisopropanolamine (DIPA) is being neglected especially in the Photo-Fenton process.

Other research studies with different degradation material have covered the affecting parameters for example; concentration of hydrogen peroxide solution, concentration of material, concentration of ferrous reagent, pH value, temperature and reaction time while the exception is the intensity of light; as taken in the research of Youssef S., Emna H. & Ridha A., 2012. Representation of DIPA degradation through Photo-Fenton process under visible light from Ritchie L. L. Z., 2013 only focused on the efficiency among parameters such as concentration of hydrogen peroxide solution, temperature, pH value, concentration of ferrous sulphate heptahydrate, concentration of DIPA and reaction time without the aspect of temperature variable. However, none of the current researches have been able to prove the effectiveness level of each parameter using design of experimentation. Therefore, the total of all the parameters (concentration of H_2O_2, concentration of $FeSO_4.7H_2O$, temperature, intensity of light, concentration of DIPA, pH value and reaction time) which account for the change in photo-degradation standard has not been linked together in a representation.

This shows that there is no present study which examines the effectiveness level of individual parameters towards the degradation standard of DIPA using Photo-Fenton process under visible light. Moreover, optimization levels for individual parameters, arranged accordingly to reaction kinetics resulting from design of experiment, have not been observed before. This concept ensures the optimization scale for Photo-Fenton process towards degradation of DIPA under visible light.

1.3 Objectives of Study

In accordance to the specific research study, certain objectives are characterized as the followings:-

I. To analyze four major manipulating parameters such as concentration of hydrogen peroxide solution, concentration of ferrous reagent, temperature and intensity of light which covers the aspect of degradation for Diisopropanolamine (DIPA) by means of Photo-Fenton oxidation process under visible light.

II. To evaluate each parameter variable towards the degradation standard of Diisopropanolamine (DIPA) in Photo-Fenton oxidation process under visible light through the method, design of experimentation tools.

III. To assert the optimization of parameter variables (arranged from the highest effectiveness towards the lowest effectiveness) for the photo-degradation of Diisoprapanolamine (DIPA) using Photo-Fenton under visible light.

IV. To validate the inferences with experimental data for optimization in Diisopropanolamine (DIPA) degradation through Photo-Fenton process under visible light.

1.4 Scope of Study

Within the research project, the range of examination covers different areas as summarized as the followings:-

a) Type of Amine Waste : Diisopropanolamine (DIPA), secondary amine
b) Design Parameter of Study : Manipulated Variable
    I. Concentration of Hydrogen Peroxide Solution : 0.1M – 1.0M

II. Concentration of $FeSO_4.7H_2O$: 0.1M –1.0M

III. Temperature : 25^oC – 35^oC

IV. Intensity of Light : 300W – 500W

c) Conditioning : Constant Variable

I. Concentration of DIPA : 500 ppm

II. pH Value : 3 (acidic)

III. Reaction Time : 60 minutes

d) Acid and Base Solution

I. Sulphuric Acid : 1.0M

II. Sodium Hydroxide : 1.0M

e) Calculation Unit : Chemical Oxygen Demand (COD)

f) Engineering Tools : Design Factorial Experimentation

1.5 Feasibility of Study

This research project is conducted inside the laboratory of Universiti Teknologi PETRONAS (UTP), Block 5, Lab 01. The analysis will be supported through the minimal funding of RM 250 (Ringgit Malaysia) per semester for materials used. Economic cost for the Photo-Fenton oxidation process is conserved since the measuring device and apparatus have been acquired since the previous semesters. In terms of environmental sustainability, there is no hazardous release and risk will be reduced with proper supervision. The surrounding conditions are suitable for control restriction in experimental research study. Overall, the sustainability of the research project is ensured through the protocol procedure.

1.6 Relevancy of Study

The research project aims to promote Advanced Oxidation Process (AOP). In regards to the scarce study of Photo-Fenton process, the results may serve as guidance for future references. The scope covered will optimize the parameters affecting the photolysis assisted Fenton's oxidation process which then provides a foundation where there will be assurance of reduction in cost and energy consumption for the AOP industry. The proceedings will ensure a significant establishment of AOP among the waste treatment methods. With that, the information may be advanced into vast applications of the industrial section.

2.0 LITERATURE REVIEW

2.1 Background Review

In the categorization of gaseous fossil fuels, natural gas, which is relatively low in energy content per unit volume, emits lesser quantities of greenhouse gases (GHG) than other fossil fuels (Pascoli, Femia et al., 2001). Nonetheless, natural gas is the most hydrogen–rich and has higher energy conversion efficiencies in comparison with other hydrocarbon energy resources. This leads to the necessity in the removal of acid gasses (carbon dioxide, CO_2 and hydrogen sulphide, H_2S) due to their corrosiveness and toxicity in nature. The following technologies of treatment such as absorption with water, absorption with polyethylene glycol, chemical absorption with amines, pressure swing adsorption (PSA)/ vacuum swing adsorption (VSA), membrane technology, cryogenic separation and biological removal are compared in Table 2.1.1.

Table 2.1.1: Alternatives in removing CO_2 and H_2S from natural gas stream (Ryckebosch et al., 2011)

Method	Option/ Alternative	Advantages	Disadvantages
Absorption with water		- High efficiency (>97% CH_4) - Simultaneous H_2S removal when H_2S< 300cm_3/m^3 - Capacity is amendable via pressure or temperature variation - Low CH_4 losses (<2%) - Tolerant to impurities	- Expensive investment and operation - Clogging due to bacterial growth - Possible foaming - Low flexibility towards variation of input gas
Absorption with polyethylene glycol		- High efficiency (>97% CH_4) - Simultaneous removal of organic S components, H_2S, ammonia (NH_3) , hydrogen cyanide (HCN) and water (H_2O) - Energetic more favorable than water - Regenerative - Low CH_4 losses	- Expensive investment and operation - Difficult operation - Incomplete regeneration when stripping/vacuum (boiling required) - Reduced operation when dilution of glycol with water

Chemical absorption with amines		- High Efficiency (>99% CH_4) - Cheap operation - More CO_2 dissolved per unit of volume (compared with water) - Very low CH_4 losses (<0.1%)	- Expensive investment - Heat required for regeneration, corrosion, decomposition and poisoning of the amines by oxygen (O_2) or other chemicals - Precipitation of salts - Possible foaming
PSA/ VSA	- Carbon molecular sieves - Zeolites Molecular sieves - Alumina silicates	- Highly efficient (95-98% CH_4) - Removal of H_2S - Low energy usage - High pressure - Compact technique - Small capacities - Tolerant to impurities	- Expensive investment and operation - Extensive process control needed - CH_4 losses when malfunctioning of valves
Membrane technology	- Gas/ gas - Gas/ liquid	- Removal of H_2S and H_2O - Simple construction - Simple operation - High reliability - Small gas flow treated without proportional increment in costs ▪(Gas/gas): removal efficiency: <92% CH_4 (1 step) or >96% CH_4, H_2O is removed ▪(Gas/liquid): removal efficiency: >96% CH_4, cheap investment and operation, pure CO_2 can be obtained	- Low membrane selectivity - Compromise between purity of CH_4 and amount of upgraded biogas - Multiple steps required (modular system) to reach high purity - CH_4 losses
Cryogenic separation		- Efficiency of 90-98% CH_4 - CO_2 and CH_4 in high purity - Low extra energy cost to reach liquefied biomethane (LBM)	- Expensive investment and operation - CO_2 can remain in the CH_4
Biological removal		- Removal of CO_2 and H_2S - Enrichment of CH_4 - No unwanted end products	- Addition of H_2 gas - Cannot be applied in large-scaled industries - Experimental work

2.2 Comparison of Treatment Methods

The method commonly used for treating CO_2 and H_2S in industry is chemical absorption by consuming amine solutions (Simmonds et al., 2002). With the comparison between various methods, further inference demonstrated chemical absorption process as the better alternative for H_2S removal (Hullu J. D., 2008). Purification process for natural-gas commonly practices chemical absorption with amine solution due to properties such as high removal efficiencies, selective ability for CO_2 and H_2S removal; and regeneration capability (Mckinsey Zicarai, 2003).

With additional evidence in selecting chemical absorption process as the better alternative, a series of comparison among 46 different reference papers are conducted through the research paper entitling "Comparison of Three Gas Separation Technologies consisting of Chemical Absorption, Membrane Separation and Pressure Swing Adsorption for CO_2 Capture from Power Plant Flue Gas" (Yang Hongjun et al., 2011). The graph of comparison is plotted in Figure 2.2.1.

Based on the graph tabulated, '●' represents the CO_2 avoided cost, 'Δ' signifies the CO_2 recovery, '▲' characterizes the CO_2 purity while the bracketed number '(…)' defines the reference numbering from journal papers. The first factor of CO_2 avoided cost shows that chemical absorption has the lowest expenditure, followed with the costlier pressure swing adsorption and the highest cost membrane separation. To accommodate the target of CO_2 capture in European Union, the CO_2 recovery must reach 90%; with the view that all three methods achieve the standard 90% CO_2 recovery via the Δ plotting. For CO_2 purity (▲), the chemical absorption achieves the highest rate at 95%, while membrane separation only achieves the highest rate at 77% and pressure swing adsorption achieves less than 50% with the highest rate. The conclusion is recommended that chemical absorption is the best method according to the lowest avoided cost, highest CO_2 recovery and CO_2 purity when compared with membrane separation and pressure swing adsorption.

The bracketed (45) of chemical adsorption represents European Commission, 2007; while the bracketed (8) and (3) of membrane separation signify the respective Klemes J. et al., 2005 and U.S. EIA, 2010. The pressure swing adsorption has bracketed (2) and (3) which correspondingly define the (Zhang A.L. and Fang D., 1996) and the same U.S. EIA, 2010.

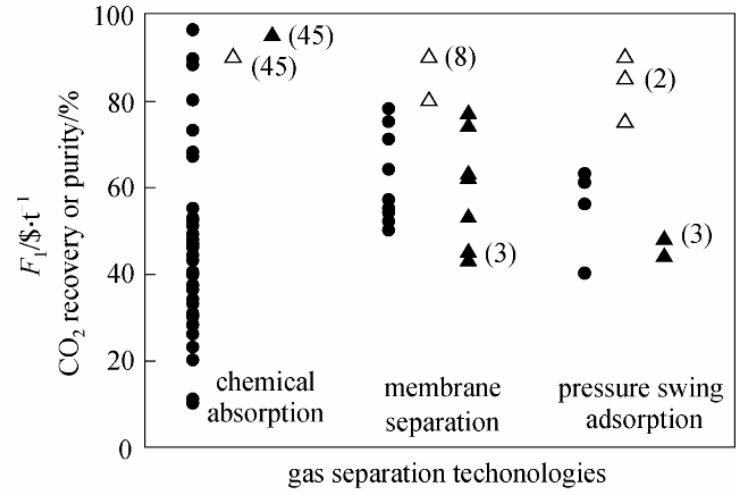

Figure 2.2.1: Comparison of chemical absorption, membrane separation and pressure swing adsorption through 46 different references
(Yang Hongjun et al., 2011)

2.3 Chemical Absorption Method

Amine treating has been a proven technology in the removal of CO_2 and H_2S through absorption and chemical processes. Amine gas treating refers to acid gas removal or gas sweetening, based on removal of acid gasses consisting of carbon dioxide, hydrogen sulphide and sulphur dioxide, by using aqueous solutions of various alkanolamines ; with the likes of Monoethanolamine (MEA), Diethanolamine (DEA), (MDEA), (DIPA) and etc. (Thomas C., 2012).

Shell introduced the Sulfinol process which consists of the passing in the natural sour gas stream through a mixture of Sulfolane, DIPA, or Methyldiethanolamine (MDEA), and water. (e,g., Dunn, 1964; Fisch, 1977; Yogish, 1990; Macgregor and Mather, 1991; Murrieta-Guevarra et al., 1994). The corresponding acid gases include H_2S, CO_2, carbonyl sulphide (COS), carbon disulphide (CS_2) and mercaptans (thiols) are physically absorbed by sulfolane and chemically absorbed by DIPA which then “sweetens” the gas stream. Figure 2.3.1 represents the flow of a typical gas treating operation using amine solvents while Table 2.3.1 shows the characteristics and absorption capacity of commonly used industrial amines for acid gases removal processes.

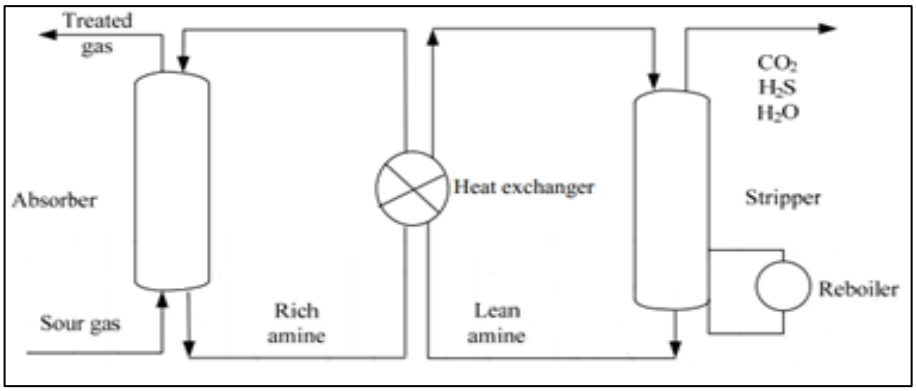

Figure 2.3.1: Schematic representation for the flow of a typical gas treating operation using amine solvents
(Kohl and Nielsen, 1997; Al-Juaied, 2004)

Table 2.3.1: Absorption capacity and some characteristics of commonly used amines for acid gases removal processes
(Kohl and Nielsen, 1997; Ritter and Ebner, 2007)

Name of amines	Vapour Pressure (mmHg)	Relative Acid Gas Capacity (%)	Remarks
Ethanolamine/ Monoethanolamine (MEA)	1.0500	100	Good thermal stability, slow losses of alkanolamine but difficult to use MEA to meet pipeline specifications for H_2S.
Diethanolamine (DEA)	0.0580	58	Lower capacity than MEA, reacts more slowly.
Triethanolamine (TEA)	0.0063	41	Low reactivity towards H_2S.
Hydroxyethanolamine/ Diglycolamine (DGA)	0.0160	58	Same reactivity and capacity as DEA, with a lower vapour pressure and lower evaporation losses.
Diisopropanolamine (DIPA)	**0.0100**	**46**	**Selective for H_2S removal over CO_2 removal.**
Methyldiethanolamine (MDEA)	0.0061	51	Selectively removes H_2S in the presence of CO_2, has good capacity, good reactivity and very low vapour pressure, a preferred solvent for gas treating.

2.4 Diisopropanolamine (DIPA)

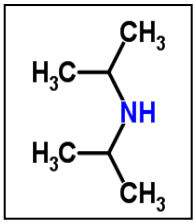

Figure 2.4.1: Molecular structure for Diisopropanolamine(DIPA) (Chemspider, 2014)

By means of previous elaborations in DIPA usage for absorption method, DIPA also plays an important role in alkanolamine-based acid gas removal (AGR) or "gassweetening process" (Sorensen et al., 1996). The reaction (AGR process) between weakly basic alkanolamines and gaseous acid produces salts, which are later removed through gas stream. Thereby, thermal regeneration decomposes amine salt in a sequential period. The main reasoning for usage of DIPA in gas sweetening process is H_2S selectivity removal (Goar and Arrington, 1979).

Diisopropanolamine (DIPA) is an aminoalcohol that belongs to the group of alkanolamines. It is a colourless liquid or white-to-yellow crystalline solid with an odour of ammonia. The overall chemical properties of DIPA are shown in Table 2.4.1.

Table 2.4.1: Chemical properties of DIPA (Hazel Mercantile Limited, 2007)

No.	Chemical Properties	Value
1	Vapor Pressure	0.02 mm Hg @ 42°C
2	Viscosity	1.98 poise @ 45°C
3	Boiling Point	249 – 250 °C @ 760 mm Hg
4	Freezing/ Melting Point	33°C (91.40°F)
5	Auto-ignition Temperature	370°C
6	Flash Point	126°C
7	Explosion Limits (Lower)	1.10 vol%
8	Explosion Limits (Upper)	5.40 vol%
9	Solubility in Water	870 G/L @ 20°C
10	Molecular Formula	$C_6H_{15}N$
11	Molecular Weight	133.19 g/mol
12	Specific Gravity/ Density	1.00398 g/cm^3

2.5 Advanced Oxidation Process (AOP)

Advanced Oxidation Processes (AOPs) have been related with the aqueous phase oxidation processes which are based mainly on the intermediacy of the hydroxyl radical (•OH) in the mechanism resulting in the destruction of the target pollutant or contaminant complex. The concept of "Advanced Oxidation Process" was established by Glaze et.al. (1987). The technology of hydroxyl radicals manages to accelerate and improves the non-selective oxidation which leads to the possibility of destructing a wider range of organic and inorganic contaminants in the solution (Kim, 2004). In regards with the high oxidative capability and efficiency, AOP is categorized as one of the popular techniques used in tertiary waste treatment (Oppenländer, 2003) which is another advanced step to remove stubborn or micro-sized contaminants that cannot be eliminated during the secondary waste treatment (Siemens, 2011). The presence of seven chemical principles towards the necessity of advanced oxidation process (AOP) can be segregated into three methodologies (Oppenländer, 2003) which are shown as the following:-

I. Initiation - Formation of hydroxyl radicals (•OH)
II. Propagation - (•OH) attacks and break molecules into smaller fragments
III. Termination - (•OH) recombine together and form water molecule (H_2O)

Hydroxyl radical (•OH) has strengthens its significance due to its powerful and non-selective chemical oxidant that reacts very rapidly with most organic compounds. Nonetheless, fluorine gas has a higher electronegative oxidation potential but it is not used in water treatment.

Table 2.5.1: Relative oxidation power of some oxidizing species (Ullmann's, 1991)

Oxidation Species	Oxidation Potential, eV
Fluorine	3.06
Hydroxyl Radical	**2.80**
Nascent Oxygen	2.42
Ozone	2.07
Hydrogen Peroxide	1.77
Perhydroxyl Radical	1.70
Hypochlorous Acid	1.49
Chlorine	1.36

With many systems qualifying under the broad definition of AOP, these systems are listed with the category of non-photochemical and photochemical reaction. The specific methods have high rates of pollutant oxidation, high flexibility concerning water quality variations and small dimension of equipment. However, the main disadvantages are relatively high treatment costs and special safety requirements because of the usage of very reactive chemicals (ozone, hydrogen peroxide), etc., and high-energy resources (UV lamps, electron beams, radioactive sources) (Kochany and Bolton, 1992).

Table 2.5.2: List of typical AOP systems (Huang et al., 1993)

Non-photochemical	Photochemical
O_3 / OH^-	H_2O_2 / UV
O_3 / H_2O_2	O_3 / UV
O_3 / US[a]	O_3 / H_2O_2 / UV
O_3 / GAC[b]	**H_2O_2 / Fe^{2+} (Photo-Fenton)**
Fe^{2+} / H_2O_2 (Fenton System)	UV / TiO_2
Electro-Fenton	H_2O_2 / TiO_2 / UV
Electron Beam Irradiation	O_2 / TiO_2 / UV
Ultrasound (US)	UV / US
H_2O_2 / US	-
O_3 / CAT[c]	-

2.6 Fenton Reaction

Fenton's treatment is founded by M.J.H. Fenton back in the year of 1984, when the technology is proven that ferrous ion (Fe^{2+}) actually promotes oxidation process with the presence of hydrogen peroxide (H_2O_2) (Montserrant Pèrez, 2002). Fenton process operates in the oxidation concept through generation of highly reactive hydroxyl radicals. The chemical equation shown below will summarize the production factor in Fenton Reaction.

$$Fe^{2+} + H_2O_2 \rightarrow Fe^{3+} + OH^- + \bullet OH \qquad (2.6.1)$$

Hydroxyl radicals are generated once the H_2O_2 is being added into a ferrous salt solution containing iron(II) ions (Fe^{2+}). A common salt solution, ferrous sulphate ($FeSO_4$) will be used as a ferrous reagent because of large quantity and non-toxic element (Stasinakis, 2008). The production of hydroxyl radicals from ferrous reagent is relatively easier since no specific reactants and apparatus are needed to perform such conditioning (R. Andreozzi, 1999). Hydrogen peroxide is chosen as one of the Fenton reagent due to its easy-handling procedure and breaking down of contaminants into environmentally benign products (Jordi Bacardit, 2007). Most suitable conditions from several research studies provide pH value ranging from 2-4, ambient temperature varying from 25°C to 35°C and the pressure of 1 atm.

In terms of industrial treatments such as aromatic, hydrocarbons, amines, phenol, polycyclic aromatics, alcohol, mineral oils and etc, Fenton's reagent is highly recommended due to its effectiveness. The Figure 2.6.1 below represents the schematic system of Fenton's reaction.

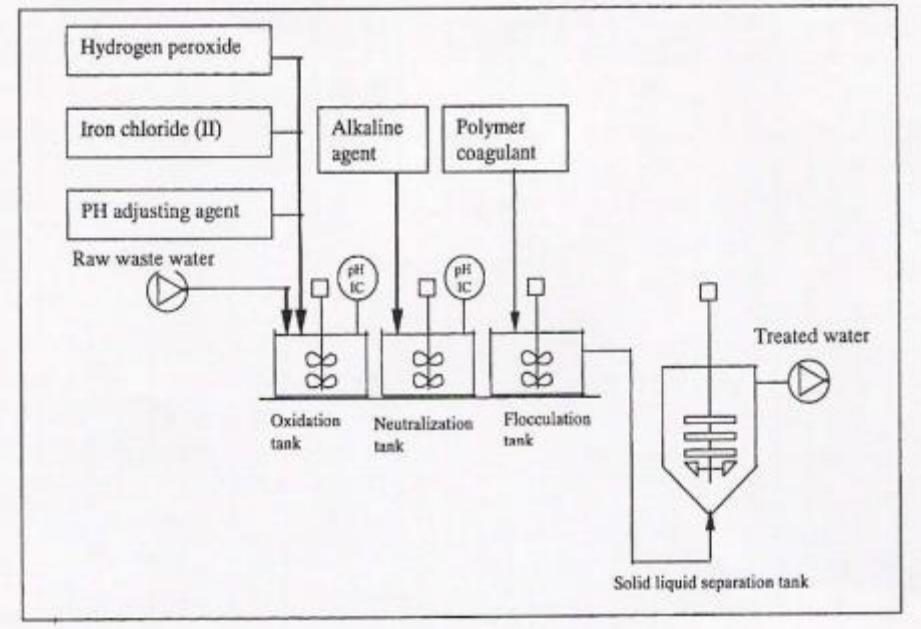

Figure 2.6.1: Scheme of the Fenton oxidation treatment (Gogate and Pandit, 2004)

2.7 Photo-Fenton Reaction

The Photo-Fenton system which consists in the combination of hydrogen peroxide (H_2O_2), ferrous iron (Fe^{2+}) and UV irradiation (Will et al., 2004) has been largely studied for the oxidation of wastewaters containing highly toxic organic compounds. (Moraes et al., 2004a,b; Legrini et al., 1993; Mansilla et al., 1997). About two decades ago, the irradiation of Fenton reaction systems with UV/Visible light is found to strongly accelerate the rate of degradation in the variation of pollutants (Huston and Pignatello, 1999; Ruppert et al., 1993). The process steps can be summarized in Figure 2.7.1.

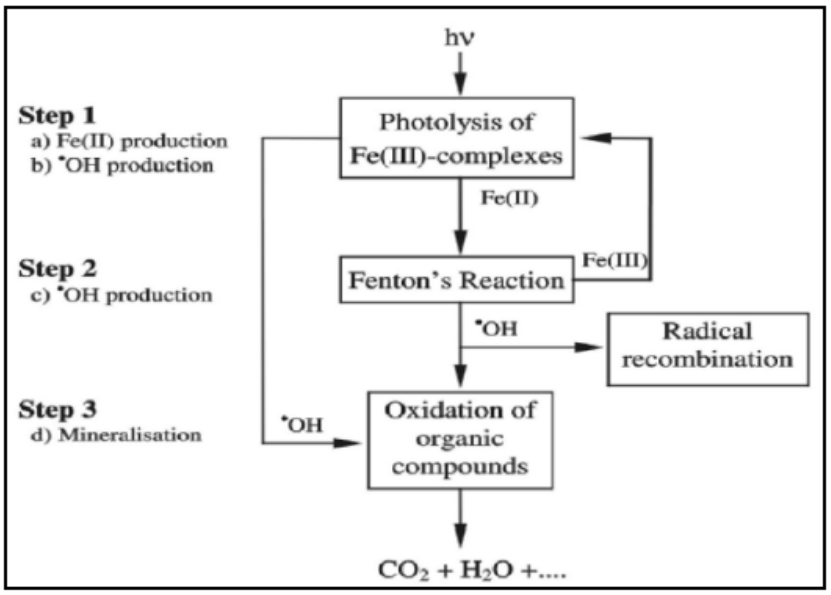

Figure 2.7.1: Reaction path of Photo-Fenton process
(A.Vogelpohl. and S.M. Kim, 2004)

After-product of Fenton reaction, Fe(III) complexes will absorb UV energy from the irradiation of UV-VIS light source and go through photolysis by producing Fe(II) ions (Fe^{2+}) and hydroxyl radical (OH) respectively.

$$Fe(OH)^{2+} + h\nu \rightarrow Fe^{2+} + \bullet OH \qquad (2.7.1)$$

Photolysis of the Fe(III) complexes will drive to the production or regeneration of Fe(II) reagent which is used to further produce hydroxyl radicals for chain oxidation processes (Kim, 2004).

$$Fe^{2+} + H_2O_2 \rightarrow Fe^{3+} + OH^- + \bullet OH \qquad (2.7.2)$$

With the constant tendency of Fe(III) ions, when in excess, to form sludge by precipitation, the solution is to recycle the Fe(III) due to the reason that Fenton reaction is being catalyzed by Fe(III) as well (limiting factor).

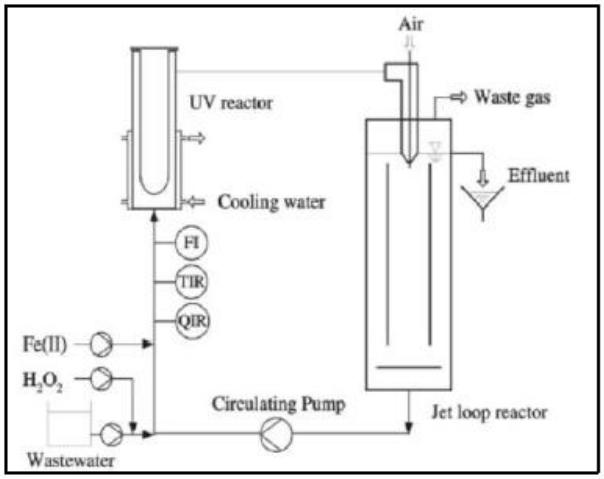

Figure 2.7.2: Example of Photo-Fenton pilot plant
(A. Vogelpohl. And S.M. Kim, 2004)

Research has been conducted to examine and compare the differences between energy cost in terms of usage and chemical price for various AOP including Photo-Fenton oxidation process. Photo-Fenton oxidation process shows the lowest reaction time for degradation while showing positive degradation efficiency of 60% TOC (Total Organic Carbon) removal. In addition to that, the total costs for energy and equipment for Photo-Fenton is much lesser when compared with other AOP treatments.

Table 2.7.1: Distribution of degradation time and costing
(Y.W. Kang and K.Y. Hwang, 2000)

Description	Degradation Time (h)	TOC Eliminated (ppm)	Chemical Costs (ATS/m^3)	Energy Demand (kWh/m^3)	Energy Costs (ATS/m^3)	Total Costs (ATS/m^3)	Total Costs (ATS/kg TOC)
Ozone	6	322 (59%)	1440	2400	3744	5184	16122
Ozone/UV	4	322 (61%)	960	2400	3744	4704	14149
UV/H_2O_2	6	71 (13%)	82	1200	1872	1954	27579
Photo-Fenton	**2.5**	**327 (60%)**	**84**	**500**	**780**	**864**	**2642**
Photo-Fenton (Sunlight)	**ca. 4**	**327 (60%)**	**84**	**0**	**0**	**84**	**257**

2.8 Cross Reference

Different articles with various suggestions and alternatives can offer multiple insights in theories and parameter investigation towards the specific research paper. The scope of study regarding the manipulated variables and constant variables are compared in terms of minimum value, maximum value and optimum conditioning. Each parameter will be studied thoroughly for the division into either manipulated or constant factor.

The degradation of chlorpyrifos insecticide in wastewater through Fenton (H_2O_2/ Fe^{2+}) and solar Photo-Fenton (H_2O_2/ Fe^{2+}/ solar light) processes are investigated in laboratory-scale (Youssef S., Emna H. & Ridha A., 2012). The degradation rate is strongly dependent on parameters such as pH value, H_2O_2 (hydrogen peroxide) dosing rate, concentration of Fe^{2+}, temperature and concentrations of chlorpyrifos insecticide. The calculations in reaction kinetics of organic matter decay are evaluated by a pseudo-second-order rate equation with respect to chemical oxygen demand (COD) measurement. The methodology started with the usage of parameters at normal conditions, such as concentration of H_2O_2 at 120mg/min, concentration of Fe^{2+} at 2.0mM, pH value at 3, concentration of chlorpyrifos at 1330mg/L and temperature at 25^{o}C. The procedure is then preceded with the optimization of parameters accordingly from each phase.

Based on Figure 2.8.1 below, the order started with the parameter, concentration of H_2O_2, which is considered to be the major effective parameter. The specific parameter is manipulated with concentrations (mg/min) consisting of 30, 60, 90, 120, 150 and 180. The highest percentage removal of COD is attained at 70 minutes when the dosing rate is of 120 mg/min. Excessive H_2O_2 reacts with OH^- ions in competition with organic pollutants which consequently reduce treatment efficiency. Therefore, optimization conditioning is concurred with the specific concentration of H_2O_2 at 120mg/min.

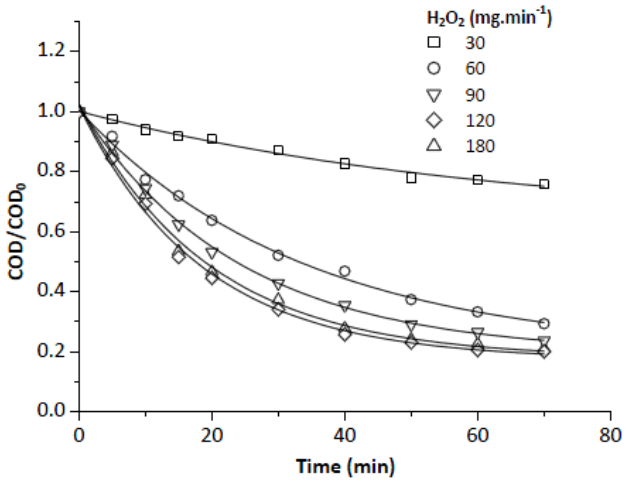

Figure 2.8.1: Effect of concentration of H_2O_2 towards COD measurement ([Chlorpyrifos]$_0$ = 1330mg/L, [Fe^{2+}]$_0$=2.0mM, pH$_0$ = 3, T$_0$ = 25^{o}C) (Youssef S., Emna H. & Ridha A., 2012)

The next parameter is based on the Figure 2.8.2 which calculates the concentration of chlorpyrifos insecticide towards the COD measurement. The process is set at normal conditions except for the concentration of H_2O_2 which is now optimized at 120 mg/min. The COD measurement showed less reduction with the increment in concentration of chlorpyrifos insecticide due to the constant hydroxyl radicals' production level with production time. Therefore, the parameter of study is set at 1330 mg/L for better research values.

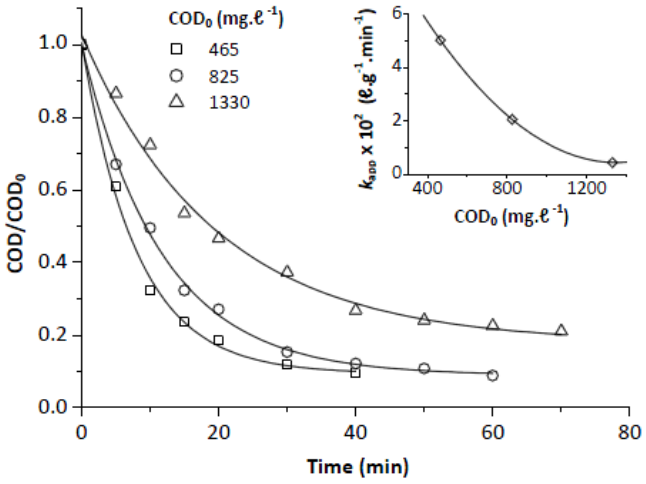

Figure 2.8.2: Effect of concentration of chlorpyrifos towards COD measurement ([H_2O_2]$_1$=120mg/min, [Fe^{2+}]$_0$ = 2.0mM, pH$_0$ = 3, T$_0$ = 25^{o}C) (Youssef S., Emna H. & Ridha A., 2012)

The procedure is continued with the concentration of Fe^{2+} towards the COD measurement as shown in Figure 2.8.3. The results showed the increment in amount of Fe^{2+} (from range of 0.5 to 5.0 mM), increases the BOD reduction value. It is due to the reasoning that Fe^{2+} has a catalytic decomposition effect on H_2O_2. However, ranges of Fe^{2+} concentrations higher than 5.0mM show decrement in COD percent removal due to competitive consumption of •OH radicals. Thus, the optimization is set at 5.0mM.

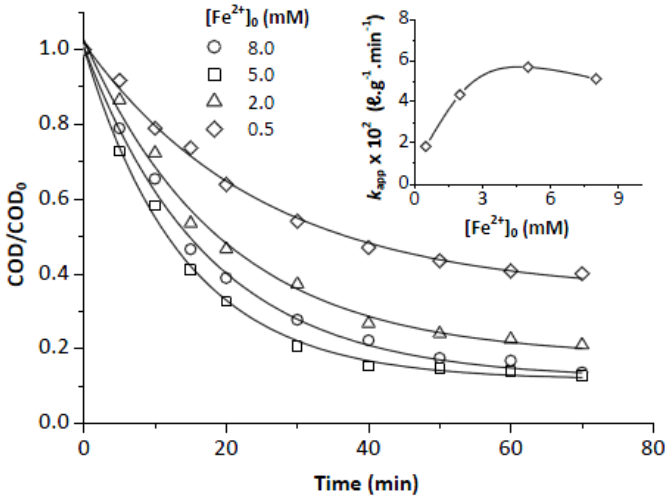

Figure 2.8.3: Effect of concentration of Fe^{2+} towards COD measurement ($[H_2O_2]_1$=120mg/min, $[Chlorpyrifos]_1$ = 1330 mg/L, pH_0 = 3, T_0 = 25°C) (Youssef S., Emna H. & Ridha A., 2012)

The next parameter optimization (Figure 2.8.4) is the pH value, which affects the oxidation of the organic substances both directly and indirectly. The pH value influences the generation of hydroxyl radicals and the oxidation efficiently. The optimum pH is found to be about 3, from the ranges of 2.5 to 4.0. The degradation decreases at pH values higher than 3.5 due to iron precipitation as hydroxide and the dissociation/auto-decomposition of H_2O_2. For pH values below 2.5, the reaction of hydrogen peroxide with Fe^{2+} is affected with the reduction in hydroxyl radical production especially in the hydroxyl-radical scavenging by H^+ ions.

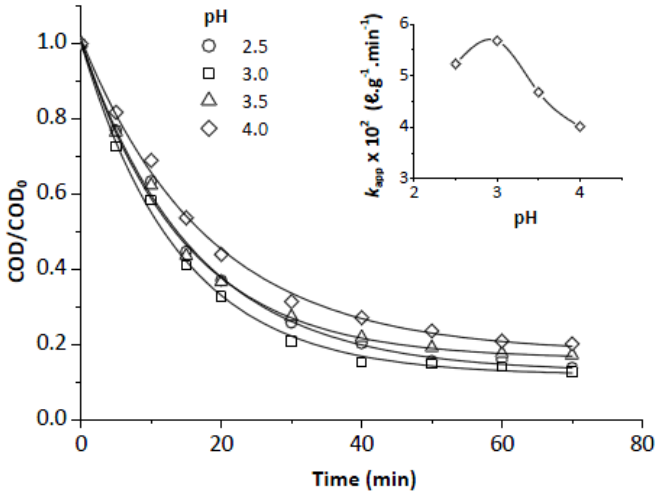

Figure 2.8.4: Effect of pH value towards COD measurement ($[H_2O_2]_1$=120mg/min, $[Chlorpyrifos]_1$ = 1330 mg/L, $[Fe^{2+}]_1$ = 5.0mM, , T_0 = 25°C)
(Youssef S., Emna H. & Ridha A., 2012)

The effect of temperature (Figure 2.8.5) is studied with temperatures range of 20, 25, 30, 35, 40 and 45°C. The results show that the k_{app} increases significantly with the reaction temperature until an optimal value of 35°C. The decrement in k_{app} at temperatures higher than 40°C is because of the accelerated decomposition of H_2O_2 into oxygen and water. Higher k_{app} value shows higher reduction in COD measurement, which means better degradation standard. The Arrhenius expression showing the relationship of reaction temperature with k_{app} is shown as the following:-

$$k_{app} = A \exp (- E_{app} / RT) \quad (2.8.1)$$

Where,

A = pre-exponential (frequency) factor

E_{app} = apparent global activation energy ($J.mol^{-1}$)

R = ideal gas constant (8.314 $J.mol^{-1}.K^{-1}$)

T = reaction absolute temperature (K)

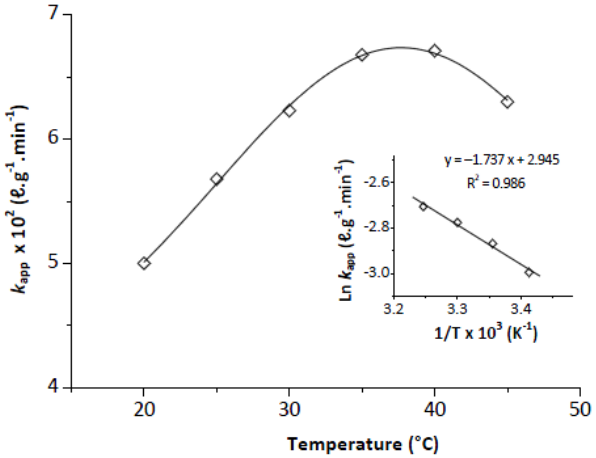

Figure 2.8.5: Effect of temperature towards k_{app} ($[H_2O_2]_1$=120mg/min, $[Chlorpyrifos]_1$ = 1330 mg/L, $[Fe^{2+}]_1$ = 5.0mM, pH_1 = 3)
(Youssef S., Emna H. & Ridha A., 2012)

The trend ratio in Figure 2.8.6 below shows that the solar Photo-Fenton system required lesser time and lesser H_2O_2 concentration to reach the same COD percent removal when compared with Fenton system. In the calculated results, the optimum experimental conditions prove that solar photo-Fenton process requires a H_2O_2 dose of 50% lower than that required in Fenton process to remove 90% of COD measurement. As shown in the smaller graph, k_{app} gradient for solar Photo-Fenton system is much steeper than the Fenton system.

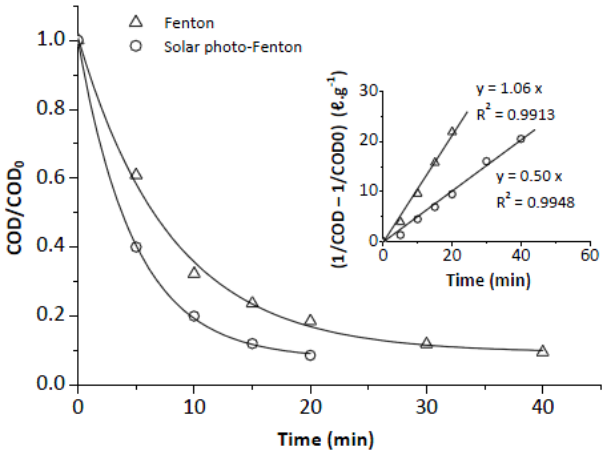

Figure 2.8.6: Fenton and Solar Photo-Fenton towards COD measurement
(($[H_2O_2]_1$=120mg/min, $[Chlorpyrifos]_1$ = 1330 mg/L, $[Fe^{2+}]_1$ = 5.0mM, pH_1 = 3, T_1= 35°C)
(Youssef S., Emna H. & Ridha A., 2012)

The optimized condition is concurred as the following Table 2.8.1:-

Table 2.8.1: Optimized conditions (Youssef S., Emna H. & Ridha A., 2012)

No.	Parameter	Conditioning
1	Concentration of H_2O_2(mg/min)	120
2	Concentration of chlorpyrifos (mg/L)	1330
3	Concentration of Fe^{2+} (mM)	5
4	pH value	3
5	Temperature (^oC)	35
6	System process	Solar Photo-Fenton

The next cross reference is almost similar in terms of achieving the efficiency of Diisopropanolamine (DIPA) degradation with different light intensities under Photo-Fenton oxidation process (Ritchie L. L. Z., 2013). The research emphasized on setting constant variables such as ferrous reagent (Ferrous sulphate heptahydrate, $FeSO_4.7H_2O$) at 0.1M, pH value at 3, temperature at 25^oC and time of 60 minutes. The manipulating variable consists of concentration of H_2O_2 which ranges from 0.1M to 1.0M, concentration of light intensity ranging from none to 500 Watt, and concentration of DIPA ranging from 100ppm to 500 ppm. The order of optimized manipulation variable will be set after each phase.

The process started with the optimization parameter for the constant variable, concentration of H_2O_2 as shown in Figure 2.8.7. The plot clearly shows the best condition where 1.0M H_2O_2 achieves nearly 50% COD removal when compared with the H_2O_2 concentrations of 0.1M and 0.01M respectively. This is due to the production of more hydroxyl radicals and the selectivity.

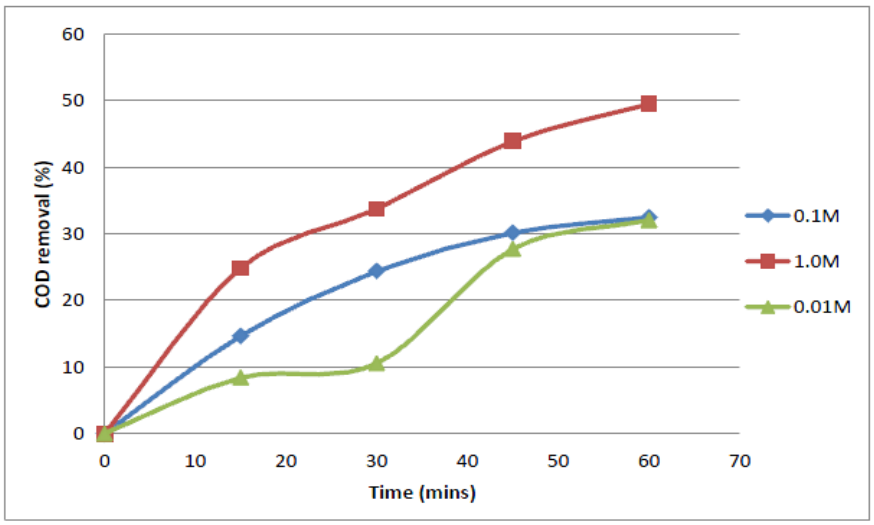

Figure 2.8.7: Effect of concentration of H_2O_2 towards COD removal (%) at 500Watt (Ritchie L. L. Z., 2013)

After the optimization for the constant variables, the methodology is preceded with the manipulation in different concentrations of DIPA towards COD removal (%) at 500Watt light intensity. The graph in Figure 2.8.8 clearly shows that the 300 ppm achieves the highest degradation standard for the corresponding factors.

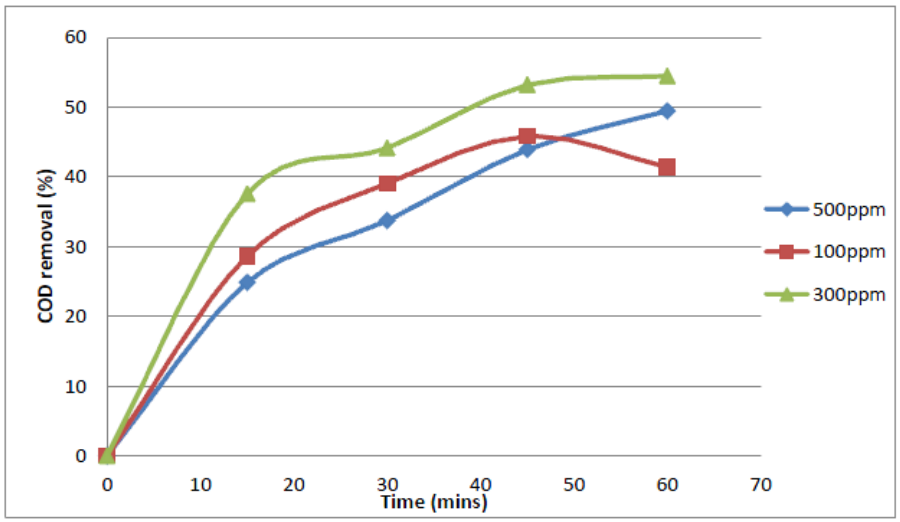

Figure 2.8.8: Effect of concentration of DIPA towards COD removal (%) at 500Watt (Ritchie L. L. Z., 2013)

The next parameter of study (Figure 2.8.9) is the light intensity at 300Watt, in which the concentration of H_2O_2 is then reexamined for the optimum conditioning. The H_2O_2 concentration of 1.0M achieves the highest COD removal (%) followed by H_2O_2 concentrations of 0.1M and 0.01M respectively. The results showed similar optimization during the light intensity of 500Watt.

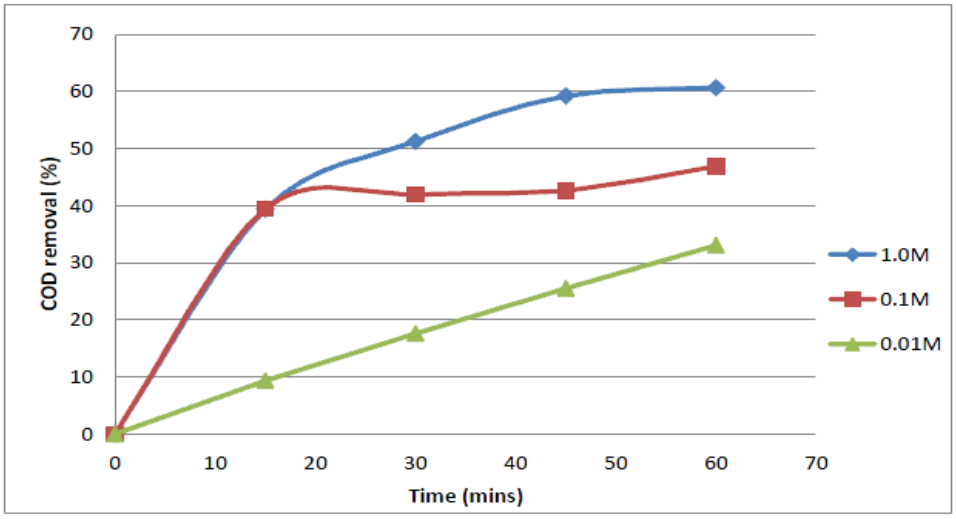

Figure 2.8.9: Effect of concentration of H_2O_2 towards COD removal (%) at 300Watt (Ritchie L. L. Z., 2013)

Later onwards, the concentration of DIPA towards COD removal (%) at 300Watt is studied as shown in Figure 2.8.10. The overall results showed that 500ppm of DIPA has the highest COD removal (%) which coincides with the inference that increment of initial DIPA concentration will relatively lead to a higher degradation standard. The low performance for degradation of 500ppm DIPA in 500Watt happened due to the possible evaporation of reaction solution as high heat energy is emitted through 500Watt of light intensity. The results also proved that the reaction rates for the degradation of 300ppm DIPA in 300Watt before 30 minutes are higher when compared with the 500ppm of DIPA in 300Watt before 30 minutes. However, the hypothesis depends on the study of reaction kinetics and determination of activation energy for better justification.

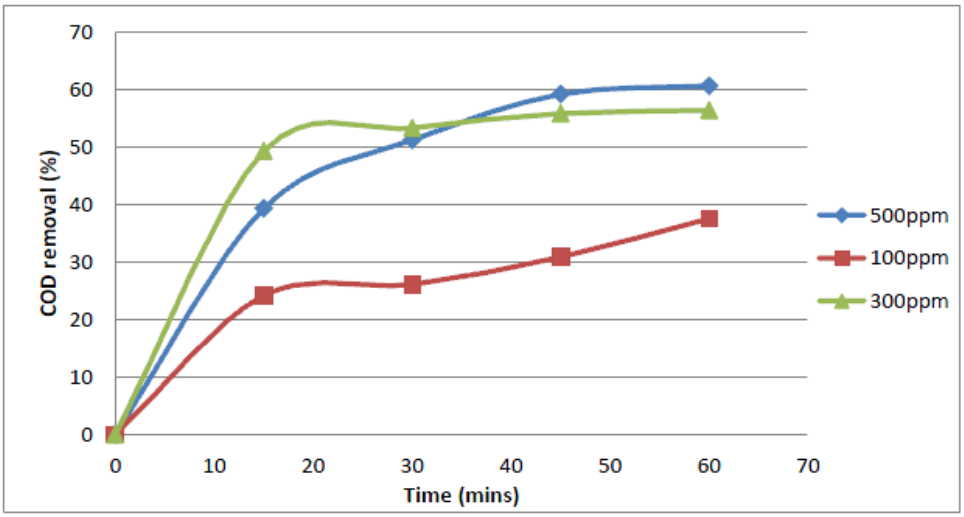

Figure 2.8.10:Effect of concentration of DIPA towards COD removal (%) at 300Watt (Ritchie L. L. Z., 2013)

The Figure 2.8.11 clearly shows the differences in trend line between the reaction systems with and without light radiation. The responding variable results are in terms of COD removal (%) with DIPA degradation under Photo-Fenton and Fenton oxidation process respectively. Both the 300ppm and 500ppm DIPA concentration under light source are much higher in COD removal (%) compared with both the 300ppm and 500ppm DIPA concentration without any light source. The significant figures prove an average of 30% COD removal. Hence, the Photo-Fenton oxidation process is evidenced to be more effective compared with the Fenton oxidation without any light source.

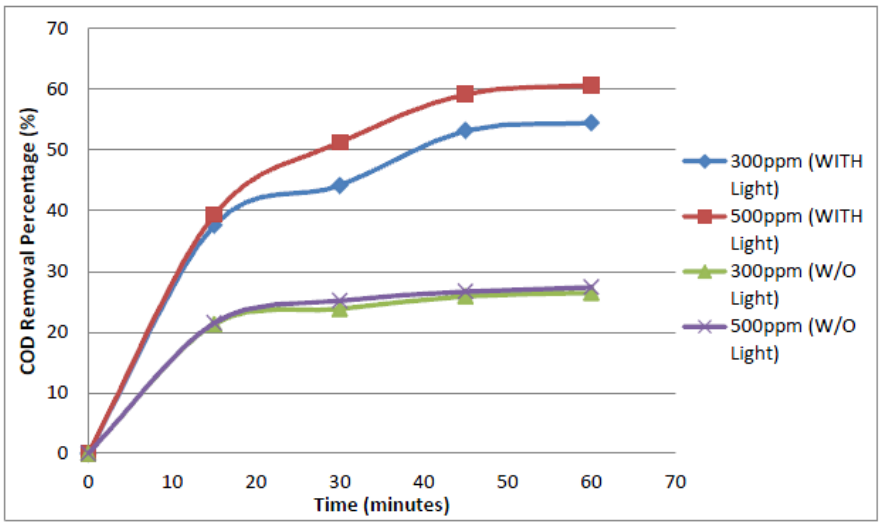

Figure 2.8.11: Comparison plot for systems with and without light (Ritchie L. L. Z., 2013)

3.0 METHODOLOGY

3.1 Experimental Approaches

The research project revolves five general approaches starting from the preparation of standard solutions such as Diisopropanolamine (DIPA), hydrogen peroxide (H_2O_2), ferrous reagent ($FeSO_4.7H_2O$), sodium hydroxide (NaOH) and sulphuric acid (H_2SO_4). The model approach then provides for the calibration of DIPA concentration curve and later onwards, move into the screening test for methodology examination. The fourth approach is the experimental design which reviews and calculates the kinetic reaction of each manipulated variable. The final approach is regarding the optimization according to the order of highest kinetic parameter variable towards the lowest kinetic parameter variable.

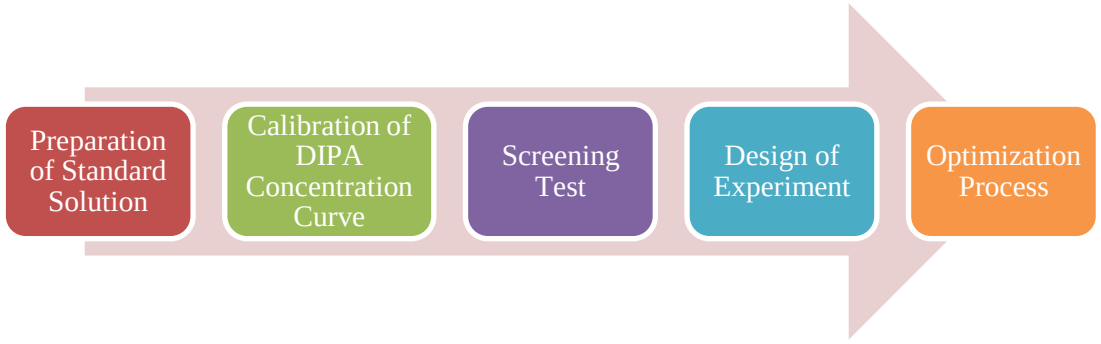

Figure 3.1.1: Experimental approaches for experimental research

3.2 Materials

The following representation exhibits the type of materials used in the conduction of research project:-

a) Type of amine waste : Secondary amine (Diisopropanolamine, DIPA , MERCK)

b) Oxidizing agent : Hydrogen peroxide (H_2O_2, 30 %, R&M Chemicals)

c) Type of ferrous reagent : Ferrous sulphate heptahydrate ($FeSO_4.7H_2O$)

d) Base solution : Sodium hydroxide (NaOH, MERCK)

e) Acid solution : Sulphuric acid (H_2SO_4, 98%, MERCK)

f) Water : Deionized water

g) Bath Fluid : Silicon oil ($350mm^2.s^{-1}$ at 25^oC, R&M Marketing-Essex U.K.)

3.3 Preparation of Standard Solutions

The classification of materials accordingly with the different preparation methods are deliberated. The materials such as DIPA solution, ferrous sulphate heptahydrate ($FeSO_4.7H_2O$), sodium hydroxide (NaOH), acids such as hydrogen peroxide (H_2O_2) and sulphuric acid (H_2SO_4) are prepared with different calculations and procedures.

3.3.1 Preparation of Amine Solution

The preparation of different concentration of DIPA solution is necessary for the calibration requirement and identification of optimum DIPA concentration for better degradation rate.

The methodology in producing different concentrations of DIPA is focused on the dilution equation, which can be divided into either the serial dilution or dilution factor. Standard solution of 1000ppm is generally prepared for the dilution cases according to the respective desired concentration. Since the concentration of 1000ppm is equivalent to 1000mg/L, 1000mg in mass of DIPA will be diluted with 1000mL (1Litre) of deionized water. The procedure is firstly preceded with the measurement of 1.0g (1000mg) of DIPA solids using an electronic weighing machine and later onwards, being dissolved with deionized water in the beaker. After the completion in dissolution of DIPA within the deionized water, the solution is then transferred into a 1Litre capacity of volumetric flask for further dilution up until 1000mL. The volumetric flask is shaken well to ensure uniform distribution of particles inside the flask.

Concentration (ppm) of DIPA solution required:-

$$1000\text{ppm} = 1000\text{mg/L}$$

$$= 1000\text{mg}/1000\text{mL}$$

Using the serial dilution and dilution factor method, the calculation for 1000ppm of standard DIPA solution is shown as the following equation:-

$$M_1V_1 = M_2V_2 \qquad (3.3.1.1)$$

Where,

M_1 = initial molarity of amine standard solution before dilution (ppm)

V_1 = initial volume of amine standard solution required for dilution (mL)

M_2 = final molarity of amine standard solution after dilution (ppm)

V_2 = final volume of amine standard solution at desired concentration (mL)

$$\text{Dilution Factor} = \frac{\text{Final Desired Volume (mL)}}{\text{Initial Required Volume (mL)}} \qquad (3.3.1.2)$$

Table 3.3.1.1: Distribution of desired DIPA concentration with respective volume

Initial Concentration M_1 (ppm)	Initial Required Volume, V_1 (mL)	Final Desired Concentration M_2 (ppm)	Final Desired Volume, V_2 (mL)	Dilution Factor
1000	350	700	500	1.43
1000	250	500	500	2.00
1000	200	400	500	2.50
1000	150	300	500	3.33
1000	100	200	500	5.00
1000	75	150	500	6.67
1000	50	100	500	10.00
1000	25	50	500	20.00
1000	15	30	500	33.33
1000	5	10	500	100.00

3.3.2 Preparation of Ferrous Reagent Solution ($FeSO_4.7H_2O$)

In the Photo-Fenton process, ferrous sulphate heptahydrate ($FeSO_4.7H_2O$) serves as the ferrous reagent which is responsible in creating hydroxyl radicals from oxidizing agent (hydrogen peroxide) for the degradation of DIPA model waste with assistance of visible light. In the design of experiment, the ferrous reagent solution ranges from 0.1M to 1.0M. With the desired range of concentration, the calculation for preparation of ferrous reagent can be done with molecular weight. The molecular weight of iron (II) sulphate heptahydrate is 278.015 g/mol. The formula for concentration calculation is shown as the followings:-

$$\text{Moles (mol)} = \text{Concentration, } M_1 \left(\frac{\text{mol}}{\text{L}}\right) \text{ x Volume, } V_1 \text{ (L)} \qquad (3.3.2.1)$$

The amount of $FeSO_4.7H_2O$ solid particles which are required are calculated with the following equation:-

$$\text{Mass of } FeSO_4.7H_2O \text{ (g)} = \text{moles (mol) x } {}^{\text{Molecular}}_{\text{Weight}} \left(\frac{\text{g}}{\text{mol}}\right) \qquad (3.3.2.2)$$

Table 3.3.2.1: Distribution of $FeSO_4.7H_2O$ calculation

Desired Concentration (mol/L)	Volume (L)	Moles (mol)	Required Mass of $FeSO_4.7H_2O$ (g)
1	1	1	278.015

3.3.3 Preparation of Sodium Hydroxide (NaOH)

Sodium hydroxide (NaOH) serves as the base solution for titration after the experimental procedures. The titration is done to filter the iron precipitates (impurities) from the after-solution for the examination of COD measurement. Moreover, the molecular weight for NaOH is 39.997 g/mol. The methods for calculation are the same as the ferrous reagent in which the molarity of NaOH will be tabulated as follows:-

Table 3.3.3.1: Distribution of NaOH calculation

Desired Concentration (mol/L)	Volume (L)	Moles (mol)	Required Mass of NaOH (g)
1	1	1	39.997

3.3.4 Preparation of H_2O_2 and H_2SO_4

The standard solution of H_2O_2 and H_2SO_4 are acidic in nature and will be differently prepared when compared with other standard solutions. The procedure will be using a burette and slowly inserting the acid into the volumetric flask (filled with deionized water) with precise calculation of volume. This is due to the higher density of acid and strong dissociation when acid reacts with water. The method of calculation is based on the serial dilution equation (3.3.1.1). The calculations will be summarized in the following table:-

$$\text{Total Concentration } \left(\frac{\text{mol}}{\text{L}}\right) = \frac{\text{Density } \left(\frac{\text{g}}{\text{L}}\right)}{\text{Molecular Weight } \left(\frac{\text{g}}{\text{mol}}\right)} \quad (3.3.4.1)$$

$$\underset{\text{Concentration}}{\text{Actual}}, M_1 \left(\frac{\text{mol}}{\text{L}}\right) = \underset{\text{at 100\%}}{\text{Total Concentration}} \left(\frac{\text{mol}}{\text{L}}\right) \times \underset{\text{Percentage}}{\text{Concentrated}} (\%) \quad (3.3.4.2)$$

$$V_1 = \frac{M_2 V_2}{M_1} \quad (3.3.1.1)$$

Table 3.3.4.1: Information for hydrogen peroxide and sulphuric acid

Material	Density (g/L)	Molecular Weight, MW (g/mol)	Total Conc. at 100% (mol/L)	Concentrated Percentage (%)	Actual Concentration, M_1 (mol/L)	Required Volume, V_1 (L)	Desired Concentration, M_2 (mol/L)	Final Volume, V_2(L)
Hydrogen Peroxide	1840	98.079	18.760	97	18.198	0.05495	1.00	1.00
Sulphuric Acid	1450	34.010	42.635	30	12.790	0.07818	1.00	1.00

3.4 Equipment and Apparatus

3.4.1 Hach DRB 200 Digester

Figure 3.4.1.1: Hach DRB 200 Digester

The equipment used to digest the samples before the measurement of COD value is Hach DRB 200 Digester. The concept procedure is the pre-heating condition until temperature of 150^{o}C and the vials (2mL of injected solution) are placed into the digester for COD digestion process under the duration of 120 minutes. The specifications and manuals will be presented in Appendix (A).

3.4.2 Hach® DR3900 Spectrophotometer

Figure 3.4.2.1: Hach® DR3900 Spectrophotometer

After the cooling down of samples which are taken out from the Hach DRB 200 Digester, the COD value is then measured by Hach® DR3900 spectrophotometer. The results such as concentration, absorbance and transmittance can be obtained. The specifications of Hach® DR3900 spectrophotometer are tabulated in Appendix (B) while the user manual is listed in Appendix (C).

3.5 Screening Test

In this approach, the screening test classifies the parameters into the manipulated and constant variable. Various series of experimental work are conducted several times to understand the importance of each parameter variable and the effect of parameter towards the degradation standard through Photo-Fenton process under visible light. Table 3.5.1 indicates the listed types of variable and their classifications.

Table 3.5.1: Parameter classifications into manipulated and constant variables

Variables	Parameter
Manipulated	a. Concentration of hydrogen peroxide solution b. Concentration of ferrous reagent c. Temperature d. Intensity of light
Constant	a. Concentration of DIPA b. Reaction time c. pH value

3.6 Design of Experiment

Design of experiment calculates the most effective parameter towards the photo-degradation standard of DIPA solution in Photo-Fenton process. The analysis involves the array of formulation 'power factor of 2' where parameters represent the power factor. Thus, there will be 16 different samplings (2^4) for the experimental conduct. Each sample will be given different conditioning to achieve the concept of modification with '-1' being the minimum range indication and '1' being the maximum range indication.

Table 3.6.1: Low and high range of factor experimentation

Parameter	Unit	Low (-1)	High (1)
Concentration of hydrogen peroxide solution (A)	mol/ L	0.1	1.0
Concentration of ferrous reagent (B)	mol/ L	0.1	1.0
Temperature (C)	^{o}C	25	35
Intensity of light (D)	Watt	300	500

Table 3.6.2: 2^4 Factorial Design Experimentation

Order	Factor A	Factor B	Factor C	Factor D
1	-1	-1	-1	-1
2	1	-1	-1	-1
3	-1	1	-1	-1
4	1	1	-1	-1
5	-1	-1	1	-1
6	1	-1	1	-1
7	-1	1	1	-1
8	1	1	1	-1
9	-1	-1	-1	1
10	1	-1	-1	1
11	-1	1	-1	1
12	1	1	-1	1
13	-1	-1	1	1
14	1	-1	1	1
15	-1	1	1	1
16	1	1	1	1

3.7 Summarized Methodology Process

500ppm of DIPA solution is prepared through dilution factor while different conditionings for the other four parameters are set at different values depending on the experimental approach. Silicon oil is used to stabilize the surrounding temperature accordingly before the beginning of Photo-Fenton process. Few drops of 1.0M H_2SO_4 are added into the model waste sample to provide an acidic condition. 5ml of H_2O_2 and $FeSO_4.7H_2O$ reagent solutions are later added with respective concentrations and placed under visible light source to undergo Photo-Fenton degradation process as shown in Figure 3.7.1. Samples are collected and monitored for COD measurement after a specified reaction time of 60 minutes.

Collected samples are titrated with NaOH solution to form ferrous precipitates and the heterogeneous mixture is then boiled to remove excess oxygen content. After that, precipitates are removed by filtration method to obtain clear

samples. 2mL of filtrated samples are transferred into COD reagent (High Concentration, HR) vials before shifting into 2 hours of digestion process through Hach DRB 200 Digester. Finally, digested samples are cooled to room temperature and measured for COD value using Hach® DR3900 spectrophotometer.

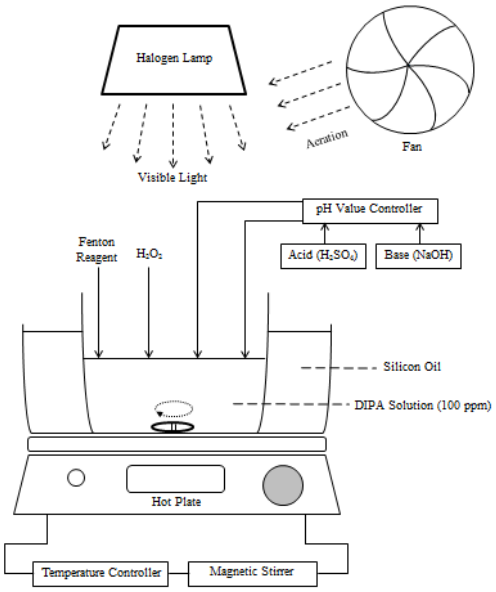

Figure 3.7.1: Schematic diagram of experimental setup

Table 3.7.1 summarizes the major types of equipment used for the experimental research with their respective function.

Table 3.7.1: Equipment usage with respective function

No.	Equipment	Function
1	Hot Plate	To provide the functions of both temperature system and stirrer system
2	Temperature System (Temperature Controller and Thermometer)	To control and to maintain the temperature of the degradation system
3	Stirrer System (Magnetic Stirrer and Magnetic Stirrer Bar)	To ascertain uniform mixing of the degradation system
4	Halogen Lamp	To provide visible light irradiation for Photo-Fenton process
5	Opaque Acrylic Sheet	To maintain ambience from surrounding light irradiation
6	Table Fan	To cool the halogen lamp

3.8 Overall Methodology Process

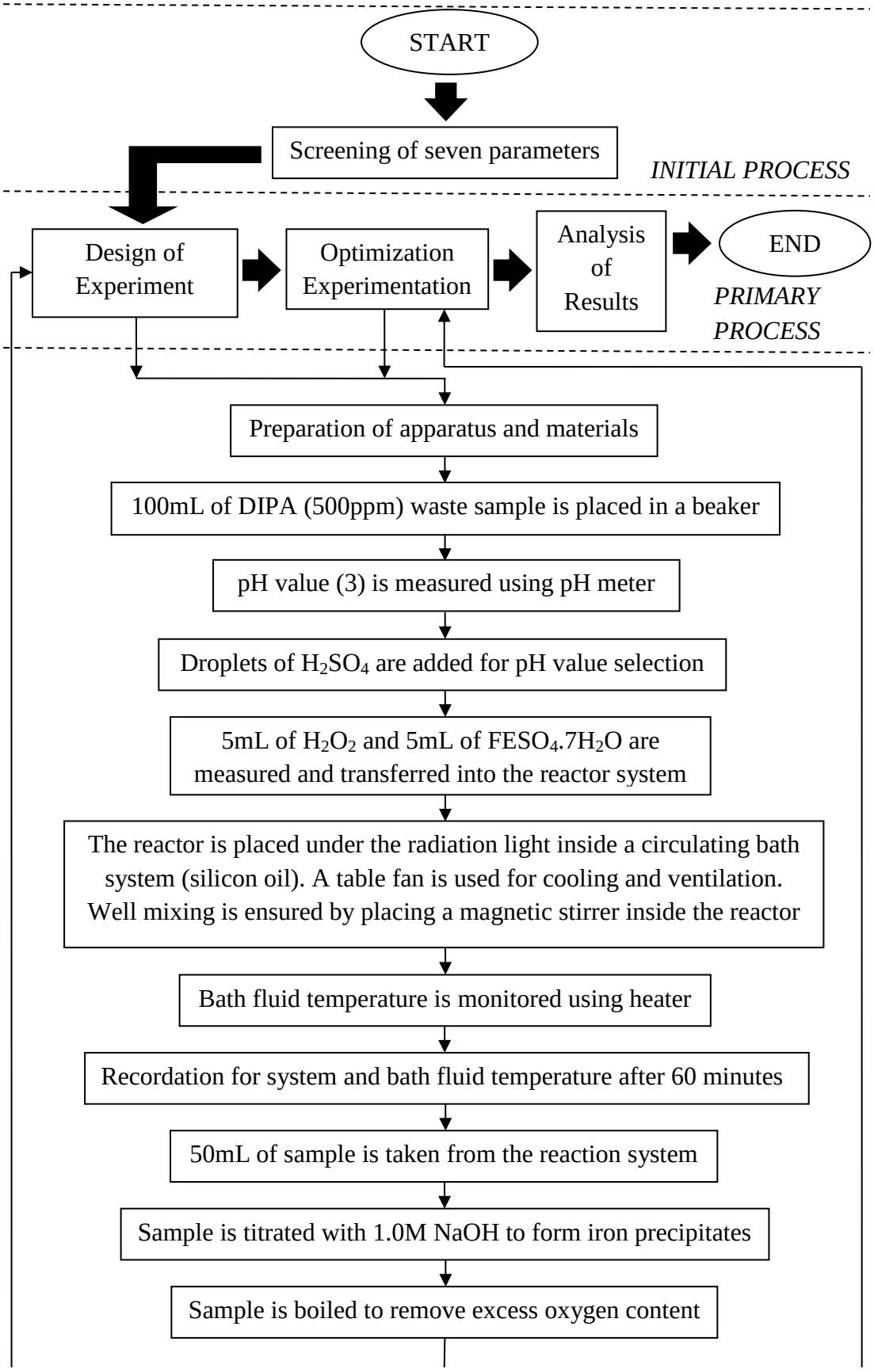

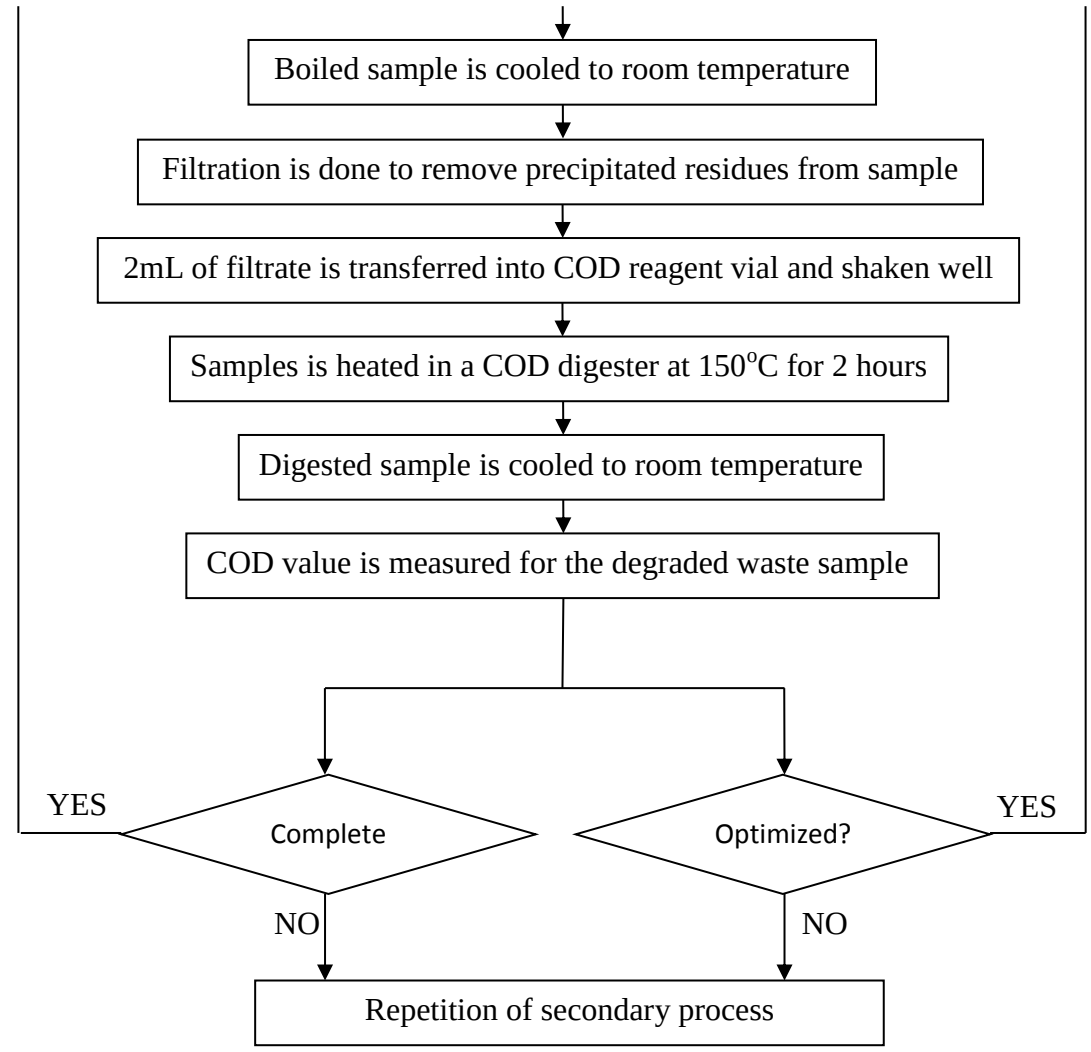

SECONDARY PROCESS

3.9 Gantt Chart

No.	Week / Description	FYP I														FYP II													
		1	2	3	4	5	6	7	8	9	10	11	12	13	14	1	2	3	4	5	6	7	8	9	10	11	12	13	14
		13/1	20/1	27/1	3/2	10/2	17/2	24/2	3/3	10/3	17/3	24/3	31/3	7/4	14/4	19/5	26/5	2/6	9/6	16/6	23/6	30/6	7/7	14/7	21/7	28/7	4/8	11/8	18/8
1	Preliminary Research Work																												
2	Preparation of Standard Solution																												
3	DIPA Sample Calibration Curve																												
4	Screening Test																												
5	2 Level Factorial Design																												
6	Optimization Parameter 1																												
7	Optimization Parameter 2																												
8	Optimization Parameter 3																												
9	Optimization Parameter 4																												
10	Analysis of Data and Conclusion																												

4.0 RESULTS

4.1 DIPA Sample Calibration Curve

With the serial dilution of Diisopropanolamine (DIPA) into various concentrations (ppm), the sample solutions are taken for Chemical Oxygen Demand (COD) testing using the Hach® DR3900 spectrophotometer. The calibration curve is plotted based on different DIPA concentrations with the respective results of COD measurement (mg/L), absorbance (abs) and transmittance (%). The purpose of the calibration curve is to compare the initial raw concentration of samples with concentration subsequent to Photo-Fenton treatment through different types of reaction system as well as reaction kinetics. The results from the measurement of various concentrations are summarized accordingly to their COD value, absorbance and transmittance in the Table 4.1.1. Overall, DIPA concentration of 500 ppm will be emphasized in this research project due to literature review and its significance factor.

Table 4.1.1: Distribution of calibration in various DIPA concentrations

DIPA Concentration (ppm)	COD Measurement (mg/L)	Absorbance (Abs)	Transmittance (%)	Dilution Factor
700	1741	0.774	16.8	1.43
500	**1302**	**0.578**	**26.4**	**2.00**
400	1031	0.458	34.9	2.50
300	759	0.337	46.1	3.33
200	487	0.216	60.8	5.00
150	353	0.157	69.7	6.67
100	253	0.112	77.2	10.00
50	115	0.051	88.9	20.00
30	47	0.021	95.3	33.33
10	13	0.006	98.6	100.00

The Figure 4.1.1 indicates the relationship between the COD measurement (mg/L) and the DIPA concentration (ppm). The trend line shows that the increment in DIPA concentration (x-axis = manipulated variable) will result in an almost similar increment in COD measurement (y-axis = responding variable). The concept is due to the increased availability for the amount of organic pollutants in the model waste which will eventually increase the concentration level where more oxygen will be consumed accordingly with the indication of COD value. In terms of proficiency, the regression R^2 of 0.9984 approaching value 1; provides a significant accuracy and consistency.

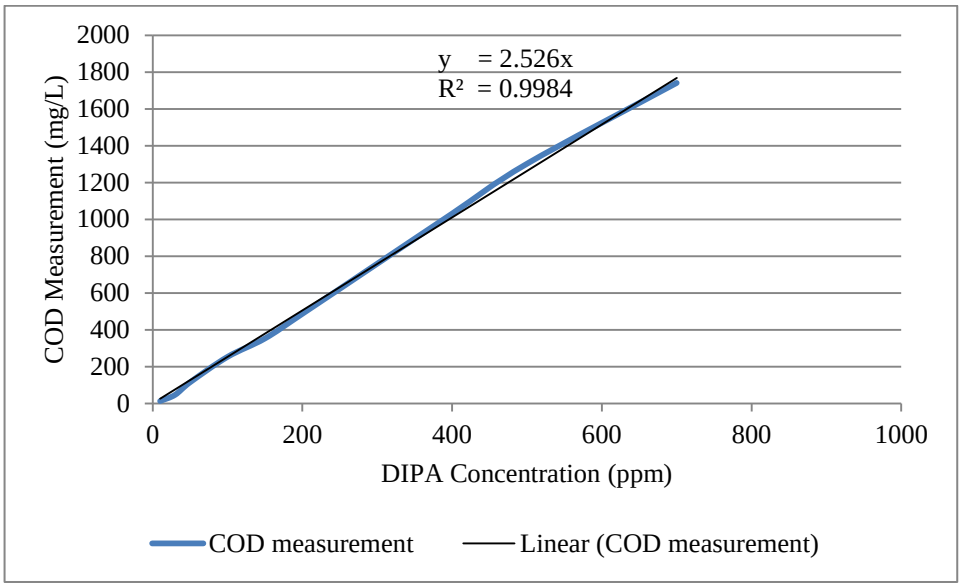

Figure 4.1.1: Calibration plot of COD measurement versus DIPA concentration

The calculation for future experimental work will be in accordance with the linear expression equation:-

$$y = 2.5246\ x \qquad (4.1.1)$$

Where,

y = DIPA concentration (ppm)

x = COD measurement (mg/L)

The Figure 4.1.2 represents the relationship of absorbance (y-axis = responding variable) against the DIPA concentration (x-axis = manipulated variable). The trend line shows a linear expression where an increment in DIPA concentration will increase the absorbance level (abs). Absorbance is defined as the index of refraction while the concept of reasoning is the same as the increment in DIPA concentration. In terms of proficiency, the regression R^2 of 0.9985 approaching value 1; provides a significant accuracy and consistency.

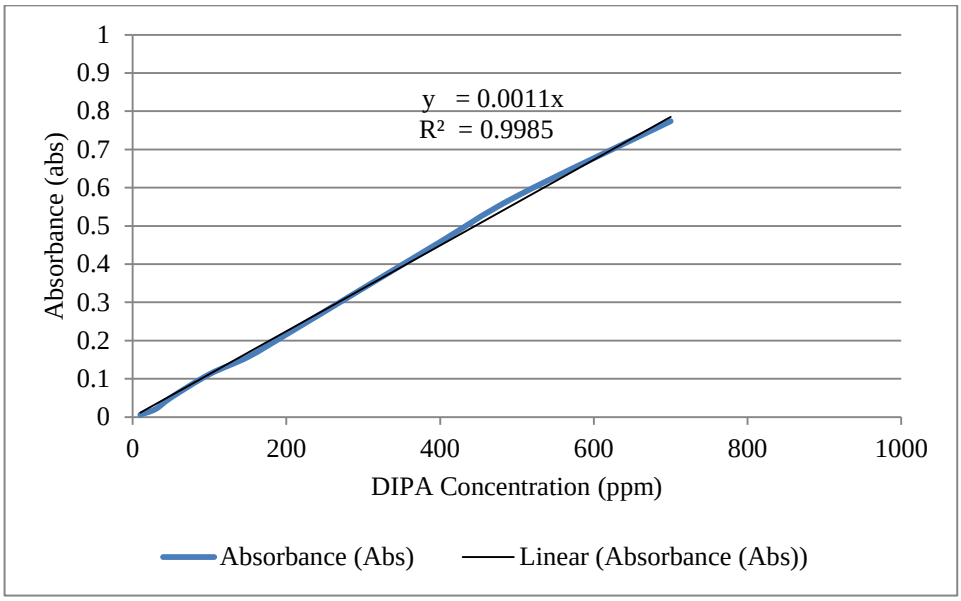

Figure 4.1.2: Calibration plot of absorbance versus DIPA concentration

The calculation for future experimental work will be related with the following linear expression equation:-

$$y = 0.0011\ x \qquad (4.1.2)$$

Where,
y = DIPA concentration (ppm)
x = absorbance (abs)

The transmittance (%) value is related with absorbance where calculations are exactly similar with the following equation:-

$$T(\%) = 10^{-(abs)}\ x\ 100\% \qquad (4.1.3)$$

Where,
abs = absorbance (abs)

4.2 Design of Experiment

Effect for significance study is carried out with different values consisting of maximum and minimum values. The experimental design are divided into several sections of analysis due to the wide range of structures.

4.2.1 Multiple Samples for Standard Order

With 16 standard orders for the examination of four different manipulating variables in Photo-Fenton process, the COD measurement(mg/L), COD removal (mg/L) and removal percentage (%) for each samples are tabulated in Table 4.2.1.1. Each parameter (Concentration of H_2O_2, concentration of $FeSO_4.7H_2O$ reagent, temperature and light intensity) are labelled with maxium and minimum range which varies differently according to different standard orders. COD removal represents the value where the COD measurement obtained with different standard orders are subtracted from the raw COD measurement (1302mg/L) obtained by 500ppm DIPA concentration in Table 4.1.1. Highest COD removal measurement was achieved by sample run 14 which is 662 mg/L (50.84% removal) while the lowest COD removal measurement was achieved by sample run 3 which is 32mg/L (2.46% removal).

Table 4.2.1.1: Multiple Samples for Standard Order of Experimental Design

No.	Concentration of H_20_2 (mol/L)	Concentration of $FeSO_4.7H_2O$ (mol/L)	Temperature (^oC)	Light Intensity (W)	COD Measurement (mg/L)	COD Removal (mg/L)	COD Percentage Removal (%)
1	0.1	0.1	25	300	1164	138	10.60
2	1.0	0.1	25	300	828	474	36.41
3	0.1	1.0	25	300	1270	32	2.46
4	1.0	1.0	25	300	892	410	31.49
5	0.1	0.1	35	300	1031	271	20.81
6	1.0	0.1	35	300	710	592	45.47
7	0.1	1.0	35	300	1233	69	5.30
8	1.0	1.0	35	300	800	502	38.56
9	0.1	0.1	25	500	1042	260	19.97
10	1.0	0.1	25	500	806	496	38.10
11	0.1	1.0	25	500	1255	47	3.61
12	1.0	1.0	25	500	878	424	32.57
13	0.1	0.1	35	500	966	336	25.81
14	1.0	0.1	35	500	640	662	50.84
15	0.1	1.0	35	500	1210	92	7.07
16	1.0	1.0	35	500	759	543	41.71

4.2.2 First Order Factorial Design

1st Order Factorial Design defines the basic and separable self-interaction among factors such as concentration fo H_2O_2 (Factor A), concentration of $FeSO_4.7H_2O$ (Factor B), temperature (Factor C) and light intensity (Factor D). Based on the plotting of data through the standard orders formed in experimental design, the effect size of single factor parameter is recorded and tabulated in Table 4.2.2.1. Positive results of effect size convey increment in COD removal (mg/L) while the negative results convey decremental rate in COD removal (mg/L). Under the advancement of +maximum values, individual factors A,C and D displays incremental positive COD removal (mg/L) while factor B shows decremental negative COD removal (mg/L).

Table 4.2.2.1: Effect size for factor A, B, C and D

Factor	Sign	Average Value	Effect Size
H_2O_2 Concentration (A)	A- (low)	155.625	-178.625
	A+ (high)	512.875	178.625
$FeSO_4.7H_2O$ Concentration (B)	B- (low)	403.625	69.375
	B+ (high)	264.875	-69.375
Temperature (C)	C- (low)	285.125	-49.125
	C+ (high)	383.375	49.125
Light Intensity (D)	D- (low)	311.000	-23.250
	D+ (high)	357.500	23.250

Figure 4.2.2.1 displays the trend line for the incremental range from lowest range (-1) to highest range (+1) for each factors. The minimum values (blue notation) represent the COD removal obtained when standard orders are presented at minimum range while the maximum values (red notation) represent the COD removal obtained when standard orders are presented at maximum range. The green notation signifies the average values from respective maximum and minimum range. In accordance to the plotted graphs, factor A has the highest incremental rate followed with C and D; lastly, a decremental rate with B.

With such arrangement, the graphs clearly divide the factors individually for further interpretation where Annova Table will be used.

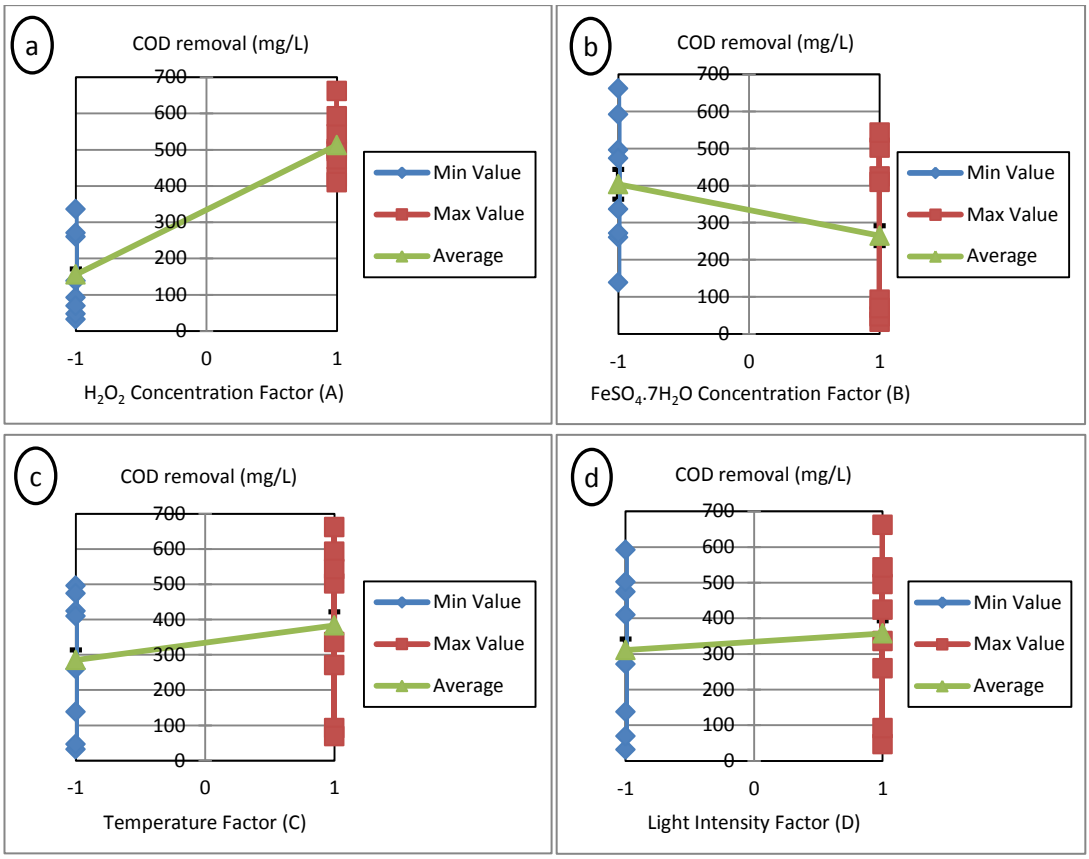

Figure 4.2.2.1: Overall graph of COD removal with (a) H_2O_2 concentration factor, (b) $FeSO_4.7H_2O$ concentration factor, (c) temperature factor and (d) light intensity factor

4.2.3 Second Order Factorial Design

The relation and interaction between two different factors are studied and listed in Table 4.2.3.1. Table 4.2.3.1 shows the effect size for six different evaluations between two factors by means of -- minimum range or ++ maximum range. Under the advancement of ++ maximum values, factor AB displays the highest positive effect size changes, followed with AC and CD; while factors AD, BC and BD shows negative effect size changes. The most significant influence is factor AB with the highest amount of effect size (±26.250); followed with factor AC (±12.750), BC (±12.500), BD (±11.625), AD (±4.875) and lastly, CD (±1.625). This reasoning shows that the interaction phase also depends on respective value in 1st Order Factorial Design; where factor A has the highest significant value. However, if the value of the opposite interaction is high, the effect size will be cancelled out due to both the opposite signs in values of interaction factor.

Table 4.2.3.1: Effect size for factor AB, AC, AD, BC, BD and CD

Factor	Average Value	Effect Size
A-B-	251.25	26.250
A+B-	556.00	-26.250
A-B+	60.00	-26.250
A+B+	469.75	26.250

Factor	Average Value	Effect Size
A-C-	119.25	12.750
A+C-	451.00	-12.750
A-C+	192.00	-12.750
A+C+	574.75	12.750

Factor	Average Value	Effect Size
A-D-	127.50	-4.875
A+D-	494.50	4.875
A-D+	183.75	4.875
A+D+	531.25	-4.875

Factor	Average Value	Effect Size
B-C-	342.00	-12.500
B+C-	228.25	12.500
B-C+	465.25	12.500
B+C+	301.50	-12.500

Factor	Average Value	Effect Size
B-D-	368.75	-11.625
B+D-	253.25	11.625
B-D+	438.50	11.625
B+D+	276.50	-11.625

Factor	Average Value	Effect Size
C-D-	263.50	1.625
C+D-	358.50	-1.625
C-D+	306.75	-1.625
C+D+	408.25	1.625

Figure 4.2.3.1 demonstrates the relation between two factors in the COD removal (mg/L) rate. The values (blue notation) represent the COD removal obtained when the 2nd factor is presented at minimum range while the values (red notation) represent the COD removal obtained when the 2nd factor is presented at maximum range. The graphs move from the left (-1, minimum values) to the right (+1, maximum values) stating the values obtained for first factor (x-axis). The different interactions prove that the effect size of the research will varies accordingly with different factors. Therefore, the graphs elaborate more on the average differences between two interaction factors rather than the true effect size.

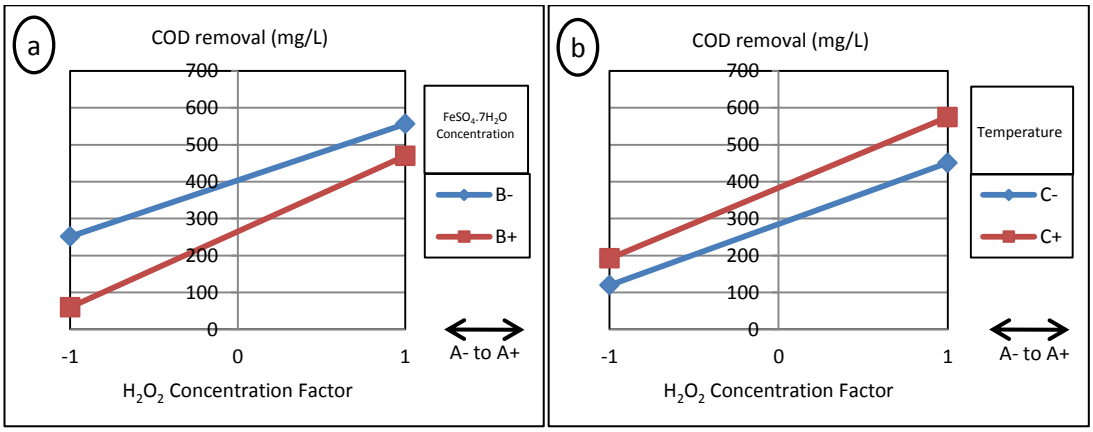

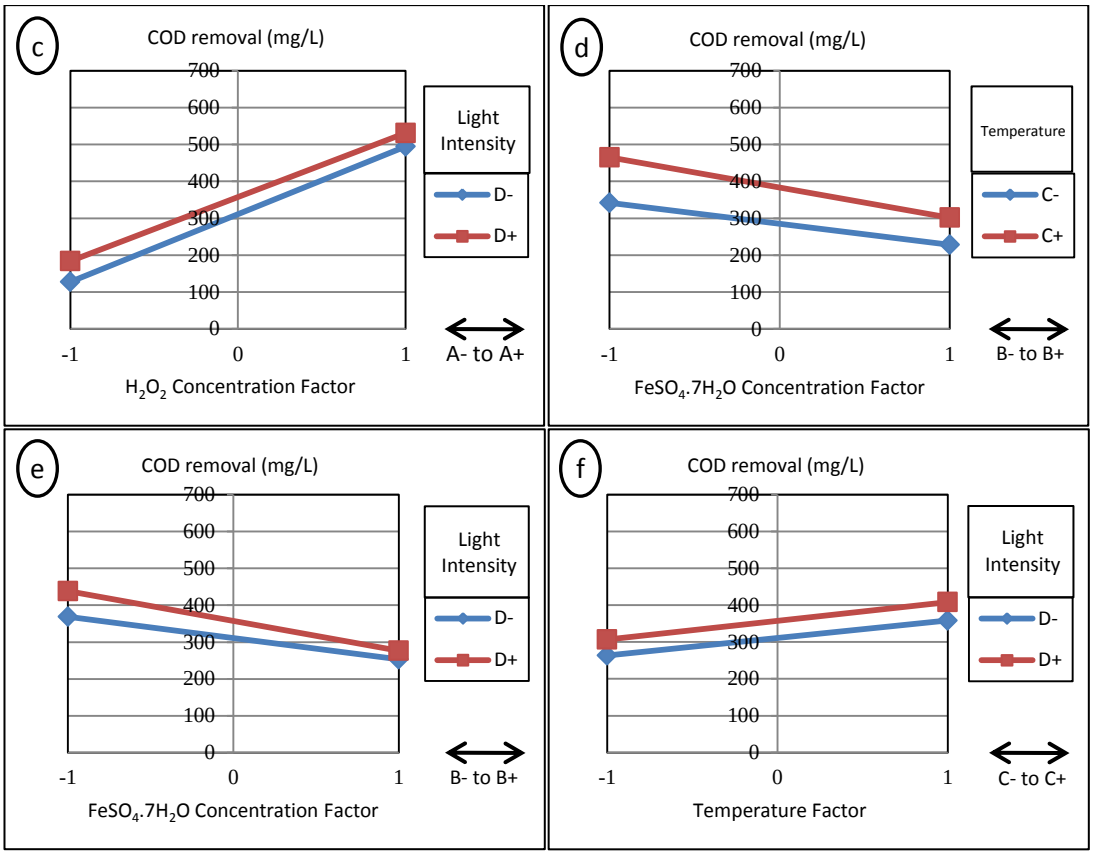

Figure 4.2.3.1: Overall graph of COD removal with (a) factor AB, (b) factor AC, (c) factor AD, (d) factor BC, (e) factor BD and (f) factor CD

4.2.4 Third Order Factorial Design

The relation and interaction between three different factors are analyzed in Table 4.2.4.1. Table 4.2.4.1 displays the effect size for four different evaluations between three factors by means of --- minimum range or +++ maximum range. Under the advancement of +++ maximum values, factor ACD displays the highest positive effect size changes, followed with ABD, ABC and BCD. All four interactions provide positive effect size changes due to the high effect of factor A; with minor reasoning due to the small positive factors of C and D. However, if the value of the opposite interaction is high, the positive effect size will be reduced due to both the opposite signs in values of interaction factor. The most significant influence is factor ABD with the highest amount of effect size (±7.750); followed with factor ABD (±7.000), ABC (±3.375) and lastly, BCD (±2.750). Graphical diagrams are not producible because of complicated three dimensional interaction points among three factors.

Table 4.2.4.1: Effect size for factor ABC, ABD, ACD and BCD

Factor	Average Value	Effect Size
A-B-C-	199.0	-3.375
A+B-C-	485.0	3.375
A-B+C-	39.5	3.375
A-B-C+	303.5	3.375
A-B+C+	80.5	-3.375
A+B+C-	417.0	-3.375
A+B-C+	627.0	-3.375
A+B+C+	522.5	3.375

Factor	Average Value	Effect Size
A-B-D-	204.5	-7.000
A+B-D-	533.0	7.000
A-B+D-	50.5	7.000
A-B-D+	298.0	7.000
A-B+D+	69.5	-7.000
A+B+D-	456.0	-7.000
A+B-D+	579.0	-7.000
A+B+D+	483.5	7.000

Factor	Average Value	Effect Size
A-C-D-	85.0	-7.750
A+C-D-	442.0	7.750
A-C+D-	170.0	7.750
A-C-D+	153.5	7.750
A-C+D+	214.0	-7.750
A+C+D-	547.0	-7.750
A+C-D+	460.0	-7.750
A+C+D+	602.5	7.750

Factor	Average Value	Effect Size
B-C-D-	306.0	-2.750
B+C-D-	221.0	2.750
B-C+D-	431.5	2.750
B-C-D+	378.0	2.750
B-C+D+	499.0	-2.750
B+C+D-	285.5	-2.750
B+C-D+	235.5	-2.750
B+C+D+	317.5	2.750

4.2.5 Fourth Order Factorial Design

Four factor variables are correlated in accordance with effect size and the interactions were listed in Table 4.2.5.1. Under the advancement of ++++ maximum values, factor ABCD shows positive effect size changes while factor ABCD shows negative effect size changes under the advancement of ---- minimum values. The effect size is ±5.375 showing that the consequence is not significant enough for the change when compared with the First (1^{st}) Order, Second (2^{nd}) Order and Third (3^{rd}) Order of Factorial Design. Therefore, the statistical analysis of 1^{st} Order Factorial Design is enough to prove the effect of significance for the research project in comparison with other factorial design.

Table 4.2.5.1: Effect size for factor ABCD

Factor	Average Value	Effect Size
A-B-C-D-	138	-5.375
A+B-C-D-	474	5.375
A-B+C-D-	32	5.375
A+B+C-D-	410	-5.375
A-B-C+D-	271	5.375
A+B-C+D-	592	-5.375
A-B+C+D-	69	-5.375
A+B+C+D-	502	5.375
A-B-C-D+	260	5.375
A+B-C-D+	496	-5.375
A-B+C-D+	47	-5.375
A+B+C-D+	424	5.375
A-B-C+D+	336	-5.375
A+B-C+D+	662	5.375
A-B+C+D+	92	5.375
A+B+C+D+	543	-5.375

4.3 Statistical Analysis

According to average factor tabulation, Table 4.3.1 displays the standardized effect, sum of squares and the percentile effect for the respective interactions. Interaction A shows the highest standardized effect, followed by factors B, C, AB, D, AC, BC, BD, ACD, ABD, ABCD, AD, ABC, BCD and finally, CD. Standardized effect defines the effect size to be doubled with both the positive/negative signs when undergoing the incremental (+, maximum) value sign. The subsequent value proves the rate whether factors have positive or negative effect to the Photo-Fenton degradation rate of DIPA. Positive standardized effect shows incremental value while negative standardized effect shows decremental value; both for COD removal in Photo-Fenton. Moreover, the ranking order is relevant to the sum of squares which are the advancement calculation for each amount of standardized effect. Higher standardized effect will increase the sum of squares which will later be converted into percentile effect.

Table 4.3.1: Standardized effect, sum of squares and percentile effect for corresponding factors

Interaction	Standardized Effect	Sum of Squares	Rank	Percentile (%)
A	357.25	5.105E^{+}5	15	77.820
B	- 138.75	77006.25	14	11.740
C	98.25	38612.25	13	5.890
D	46.50	8649.00	11	1.320
AB	52.50	11025.00	12	1.680
AC	25.50	2601.00	10	0.400
AD	- 9.75	380.25	4	0.058
BC	- 25.00	2500.00	9	0.380
BD	- 23.25	2162.25	8	0.330
CD	3.25	42.25	1	6.441 E^{-}3
ABC	6.75	182.25	3	0.028
ABD	14.00	784.00	6	0.120
ACD	15.50	961.00	7	0.150
BCD	5.50	121.00	2	0.018
ABCD	- 10.75	462.25	5	0.070

The Figure 4.3.1 shows the categorized percentile effect for all 15 interaction factors with factors. This proves that the individual 1st Order Factorial Design has the most important impact for Photo-Fenton research and will further be used for analysis.

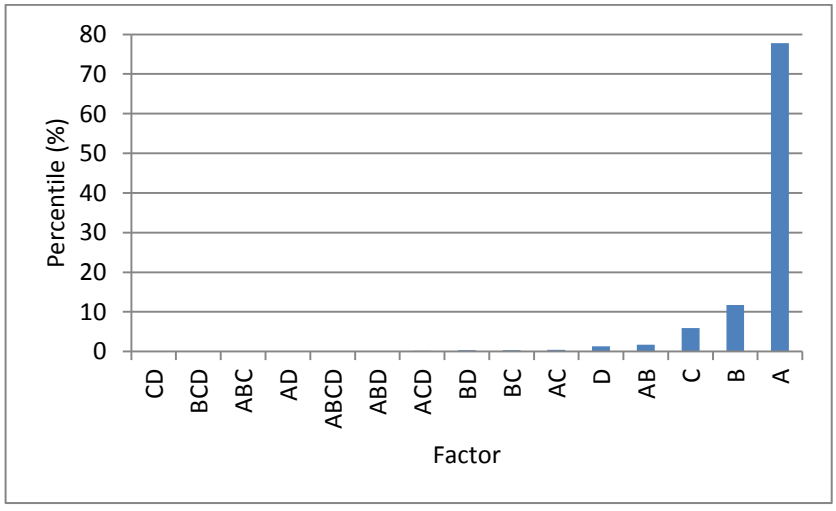

Figure 4.3.1: Percentile effect for corresponding factors

4.4 Annova Table

Based on the listings of 1st Order Factorial Design, the significant effect of individual factors are determined in Table 4.4.1. The residual represents the other remaining interaction factors that are calculated for comparison.

Table 4.4.1: Annova Table for 1st Order Factorial Design; factor A, B, C and D

Source	Sum of Squares	Degree of Freedom	Mean Square	F-Value	Probability>F
Overall	6.348E+5	4	1.587E+5	82.26	< 0.0001
A	5.105E+5	1	5.105E+5	264.62	< 0.0001
B	77006.25	1	77006.25	39.92	< 0.0001
C	38612.25	1	38612.25	20.01	0.0009
D	8649.00	1	8649.00	4.48	0.0578
Residual	21221.25	11	1929.20		
Total	6.560E+5	15			

Hypothesis : All factors are equal.

Inference : Since the overall (Probability>F) of factors A, B, C and D are <0.0001, which is lower than 0.05, the hypothesis is rejected.

Confirmation : All factors are not equal.

Statement : A, B and C are significant terms since their (Probability > F) is smaller than 0.05. D is the probable significant term with (Probability > F) smaller than 0.1 but larger than 0.05.

Deduction : Order of significant effect is arranged from highest value starting from A; closely followed with value of B, C and finally, D.

4.5 Optimization Study

With the arrangement order from highest significance towards lower significance, the optimization study are listed starting from concentration of H_2O_2 towards concentration of $FeSO_4.7H_2O$, temperature and light intensity. The most efficient range will be optimized accordingly in each parameter study beginning from the minimum conditioning onwards.

4.5.1 Optimization for Concentration of H_2O_2

In the varying parameter for concentration of H_2O_2, the minimum conditionings for all other parameters include 0.1M concentration, 25^{o}C temperature and 300Watt light intensity. Based on the Table 4.5.1.1, the raw calibration of 500ppm DIPA indicates the before-experimental material while the changing concentration of H_2O_2 directs different COD measurement. The increment in concentration of H_2O_2 until a maximum range of 1.0M provides higher COD removal (mg/L). The COD measurement (mg/L) is indirectly proportional to both COD removal (mg/L) and COD percentage removal (%). The optimized conditioning for concetration of H_2O_2 is at 1.0M while achieving percentage removal of 37.56%; differences of 25.66% between percentage removal of highest range and lowest range which is higher than 5% differences efficiency ratio. H_2O_2 acts as an oxidizing agent where any increasing concentration signifies increment in production rate of •OH radicals, which are essential in Photo-Fenton process.

Table 4.5.1.1:Optimization results for different concentrations of H_2O_2

Concentration of H_2O_2 (mol/L)	Concentration of $FeSO_4.7H_2O$ (mol/L)	Temperature (^{o}C)	Light Intensity (Watt)	COD Measurement (mg/L)	COD Removal (mg/L)	COD Percentage Removal (%)
Raw Calibration (500 ppm DIPA)				1302	-	-
0.1	0.1	25.0	300	1147	155	11.90
0.3	0.1	25.0	300	1053	249	19.12
0.5	0.1	25.0	300	968	334	25.65
0.8	0.1	25.0	300	889	413	31.72
1.0	**0.1**	**25.0**	**300**	**813**	**489**	**37.56**

Figure 4.5.1.1 shows the graph where optimization is done for different concentrations of H_2O_2. The red graph bar indicates the raw calibration of 500ppm DIPA (mg/L), the blue graph bar indicates the treated Photo-Fenton process for DIPA (mg/L) and the yellow-black line represents the COD precentage removal (%). It can be seen that increasing H_2O_2 concentration produces lower COD concentration (mg/L) while the COD removal percentage (%) increases. Optimization for the following graph is highest when concentration is at 1.0M H_2O_2 (813mg/L, 37.56%).

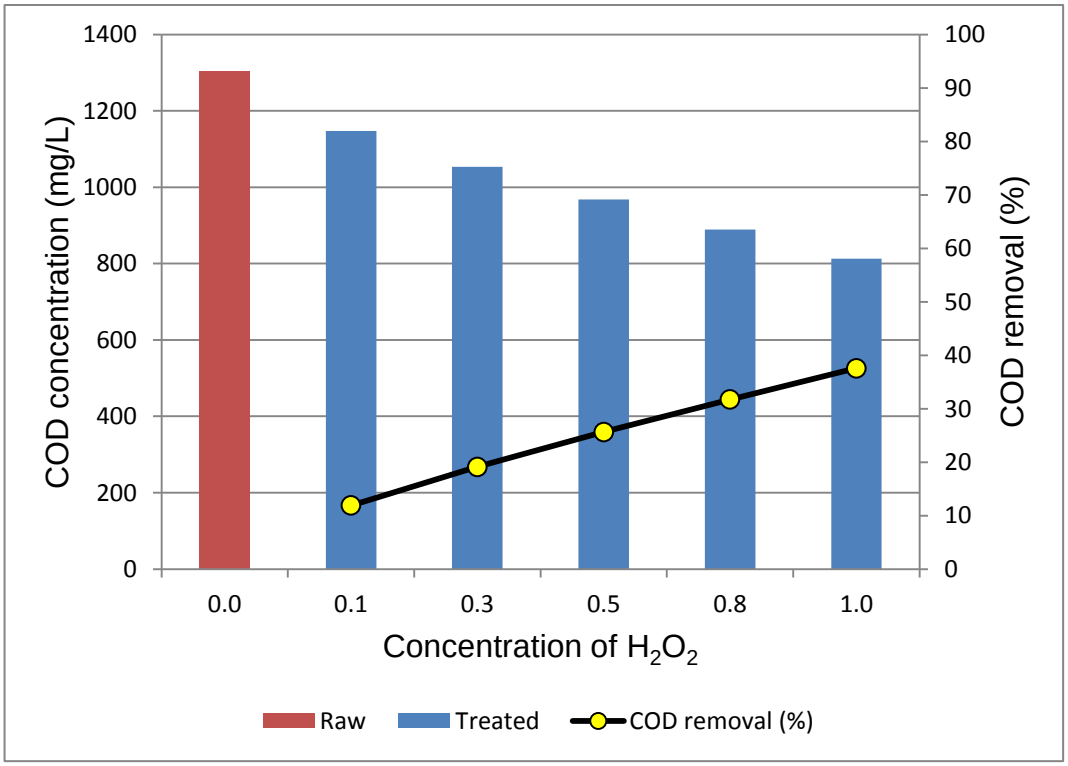

Figure 4.5.1.1: Optimization graph for different concentrations of H_2O_2

4.5.2 Optimization for Concentration of $FeSO_4.7H_2O$

The next parameter of optimization will be concentration of $FeSO_4.7H_2O$ where concentration of H_2O_2 is already optimized at 1.0M; while minimum conditioning of temperature and light intensity are at 25^{o}C and 300Watt respectively. Table 4.5.2.1 shows the varying parameter for concentration of $FeSO_4.7H_2O$ ranging from minimum range of 0.1M to maximum range of 1.0M. In comparison with the raw calibration of 500ppm DIPA, 0.5M $FeSO_4.7H_2O$ acheives the lowest COD measurement of 650mg/L and highest COD removal percentage of 50.08%. The concentration of $FeSO_4.7H_2O$ is directly related with specific concentration of H_2O_2 under regulating ratio (1:2) where production of •OH radicals are best adjusted.

Table 4.5.2.1: Optimization results for different concentrations of $FeSO_4.7H_2O$

Concentration of H_2O_2 (mol/L)	Concentration of $FeSO_4.7H_2O$ (mol/L)	Temperature (^oC)	Light Intensity (Watt)	COD Measurement (mg/L)	COD Removal (mg/L)	COD Percentage Removal (%)
Raw Calibration (500 ppm DIPA)				1302	-	-
1.0	0.1	25.0	300	815	487	37.40
1.0	0.3	25.0	300	710	592	45.47
1.0	**0.5**	**25.0**	**300**	**650**	**652**	**50.08**
1.0	0.8	25.0	300	712	590	45.31
1.0	1.0	25.0	300	884	418	32.10

According to Figure 4.5.2.1, red graph bar indicates the raw calibration of 500ppm DIPA (mg/L), the blue graph bar indicates the treated Photo-Fenton process for DIPA (mg/L) and the yellow-black line represents the COD precentage removal (%). A specific amount of ratio (0.5M:1.0M, 1:2) between $FeSO_4.7H_2O$ and H_2O_2 is the reason for achieving highest COD percentage removal of 50.08% (650mg/L). The values of 1.0M H_2O_2 and 0.5M $FeSO_4.7H_2O$ are taken for the next optimization parameter consisting of temperature.

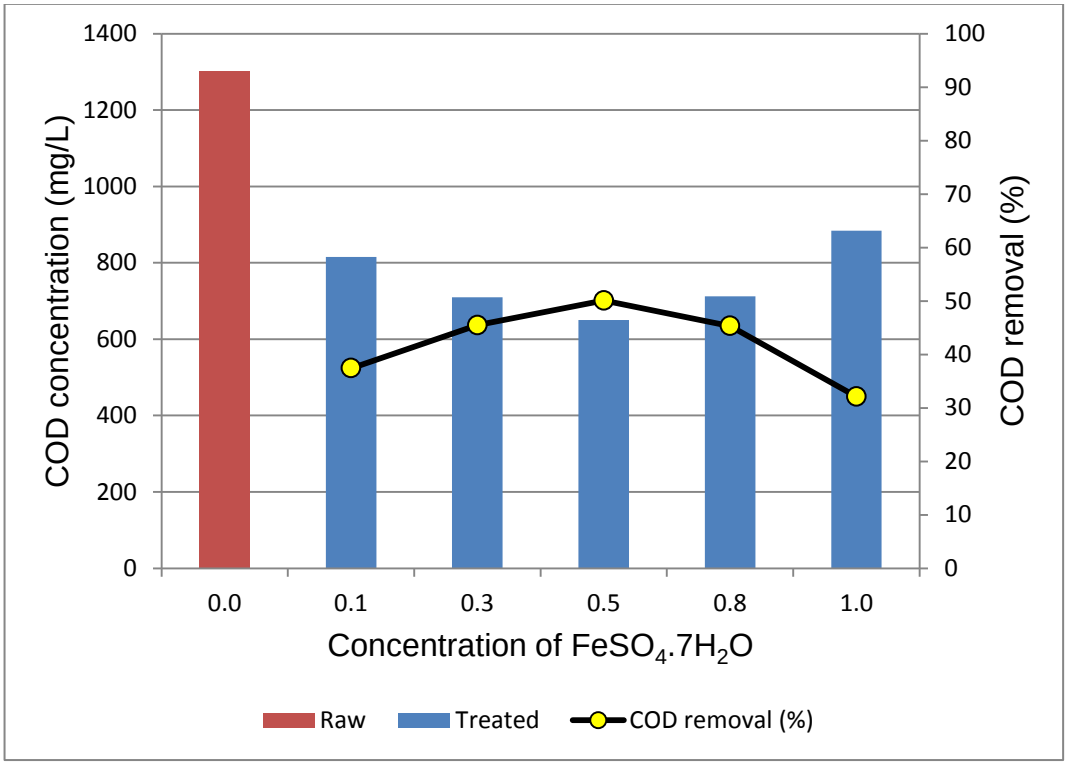

Figure 4.5.2.1: Optimization graph for different concentrations of FeSO4.7H2O

4.5.3 Optimization for Temperature

In varying temperature parameter, both concentrations of H_2O_2 and $FeSO_4.7H_2O$ are optimized at 1.0M and 0.5M respectively while light intensity is at minimum range of 300Watt. With reference to Table 4.5.3.1, the increasing temperature brings an increment in COD percentage removal (lower COD measurement, mg/L). The optimized condition is set at 35^oC where COD measurement is obtained at 531mg/L and COD percentage removal is acquired at 59.22%; differences of 8.91% between percentage removal of highest range and lowest range which is higher than 5% differences efficiency ratio. Generation of •OH radicals through oxidation process are promoted with increasing reaction temperature. The maximum range of temperature (35^oC) is set due to literature review and unfavourable conditioning towards poor stability of H_2O_2 which later affects poor •OH radicals production.

Table 4.5.3.1: Optimization results for different temperatures

Concentration of H_2O_2 (mol/L)	Concentration of $FeSO_4.7H_2O$ (mol/L)	Temperature (^oC)	Light Intensity (Watt)	COD Measurement (mg/L)	COD Removal (mg/L)	COD Percentage Removal (%)
Raw Calibration (500 ppm DIPA)				1302	-	-
1.0	0.5	25.0	300	647	655	50.31
1.0	0.5	27.5	300	619	683	52.46
1.0	0.5	30.0	300	589	713	54.76
1.0	0.5	32.5	300	558	744	57.14
1.0	**0.5**	**35.0**	**300**	**531**	**771**	**59.22**

Based on the Figure 4.5.3.1, the raw calibration of 500ppm DIPA (mg/L) is denoted with red graph bar, treated Photo-Fenton process (mg/L) is designated for blue graph bar and the COD percentage removal (%) is signified by yellow-black line. The trend line shows an incremental gradient towards increasing temperature. Temperature conditioning of 35^oC complements the local average temperature where experimental setup is conducted. Therefore, the current optimization is adjusted to 1.0M concentration of H_2O_2, 0.5M concentration of $FeSO_4.7H_2O$ and temperature of 35^oC.

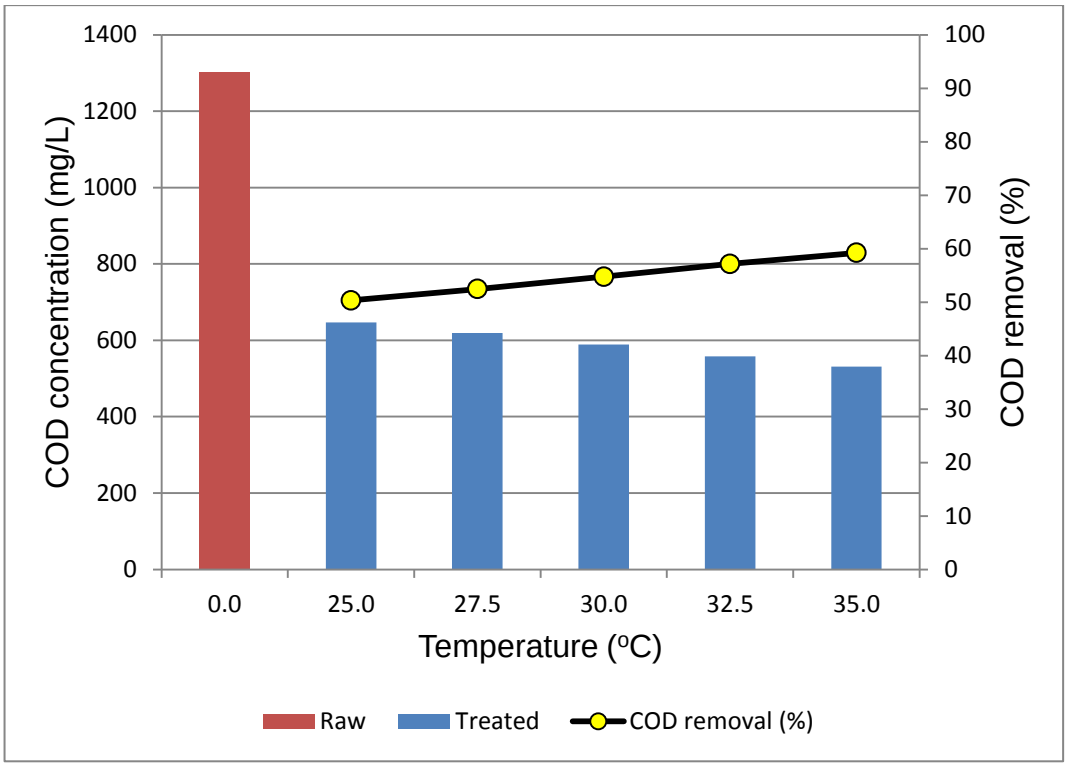

Figure 4.5.3.1: Optimization graph for different temperatures

4.5.4 Optimization for Light Intensity

The final optimization parameter is light intensity where range varies from 300 to 500 Watt; meanwhile other parameters are optimized at 1.0M concentration of H_2O_2, 0.5M concentration of $FeSO_4.7H_2O$ and temperature of 35°C. From Figure 4.5.4.1, the increasing light intensity produces increasing COD percentage removal (lower COD measurement, mg/L). Through results obtained, optimized condition is set at 300 Watt which achieves 59.22% (531mg/L) due to reason that differences of 3.38% between percentage removal of highest range and lowest range which is lower than 5% differences efficiency ratio. Therefore, cost towards effectiveness ratio of increasing light intensity to 500Watt is not liable .

Table 4.5.4.1: Optimization results for different light intensities

Concentration of H_2O_2 (mol/L)	Concentration of $FeSO_4.7H_2O$ (mol/L)	Temperature (°C)	Light Intensity (Watt)	COD Measurement (mg/L)	COD Removal (mg/L)	COD Percentage Removal (%)
Raw Calibration (500 ppm DIPA)				1302	-	-
1.0	**0.5**	**35.0**	**300**	**531**	**771**	**59.22**
1.0	0.5	35.0	350	519	783	60.14
1.0	0.5	35.0	400	507	795	61.06
1.0	0.5	35.0	450	496	806	61.90
1.0	0.5	35.0	500	487	815	62.60

Figure 4.5.4.1 shows the red graph bar which represents the raw calibration of 500ppm DIPA (mg/L) , the blue graph bar which denotes the treated Photo-Fenton process (mg/L) and the yellow-black line which signifies the COD percentage removal (%). Regardless of the incremental trend line growth, the cost towards effectiveness ratio is not sufficient for optimization increment from range 300 to 500 Watt. Overall, the optimum conditioning is set at 300 Watt where COD measurement is recorded at 531mg/L (59.22% COD percentage removal).

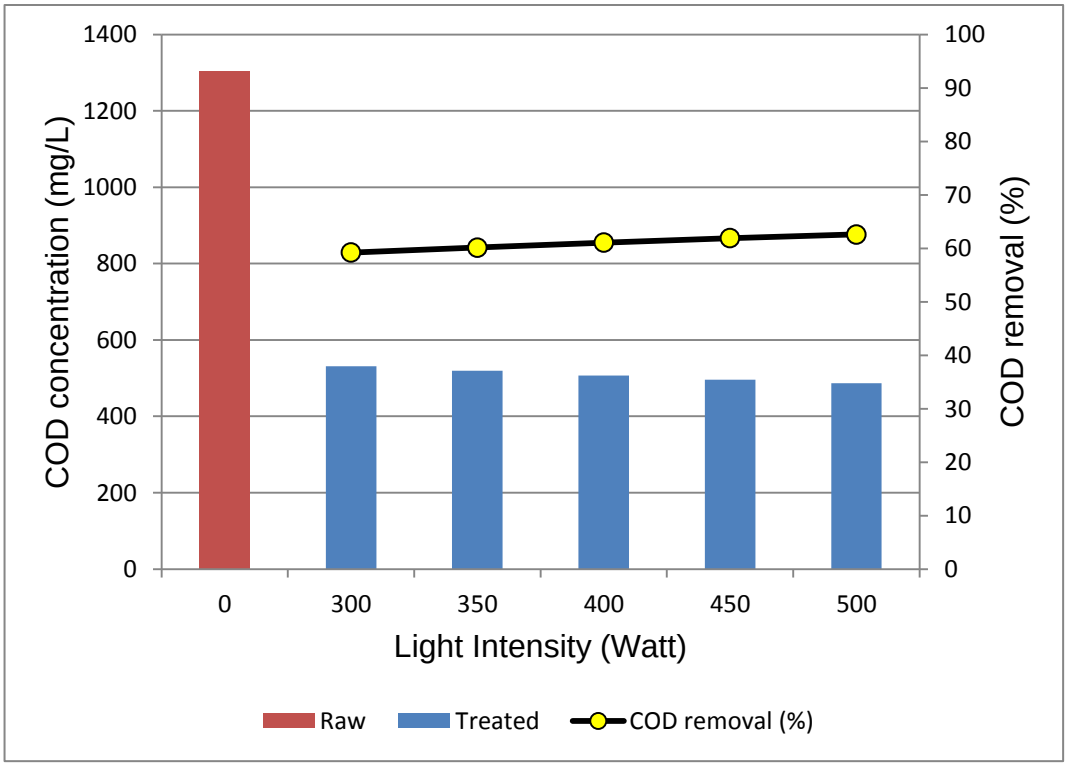

Figure 4.5.4.1: Optimization graph for different light intensities

4.5.5 Overall Optimization

In accordance with the order arranging from concentration of H_2O_2 towards concentration of $FeSO_4.7H_2O$, temperature and finally, light intensity, the optimization process is finally adjusted at its finest conditioning. With each range, the inference states the reasoning of choice especially in terms of cost, efficiency and difference in COD percentage removal of 5% between highest range and lowest range. Table 4.5.5.1 represents the overall optimization for Photo-Fenton process after following the parameter order resulting from design of experiment.

Table 4.5.5.1: Overall Optimization for Photo-Fenton process

Factor	Parameter	Condition	COD Removal	Inference
A	Concentration of H_2O_2 (mol/L)	1.0	813 mg/L (37.56 %)	Higher concentration of oxidizing agent increases production rate of •OH radicals
B	Concentration of $FeSO_4.7H_2O$ (mol/L)	0.5	650 mg/L (50.08 %)	Ratio of $FeSO_4.7H_2O$ will be directed with concentration of H_2O_2 for better efficiency of •OH radicals
C	Temperature (^oC)	35.0	531 mg/L (59.22 %)	Moderate temperature provides a suitable degradation environment for Photo-Fenton process
D	Light Intensity (Watt)	300.0	531 mg/L (59.22 %)	Higher increment of 500 Watt did not provide efficient growth in degradation rate prior to cost effectiveness
		Optimized Condition	**531 mg/L (59.22 %)**	

4.6 Comparison for Significance of Temperature and Light Intensity

Figure 4.6.1 shows the comparison graph for Photo-Fenton process with the significance in presence or absence of temperature and light intensity. Fenton reagents denote the presence of H_2O_2 and $FeSO_4.7H_2O$ solution within experimental conduct. The blue graph bar indicates the presence of all parameter (having the same results as optimization data) which achieves highest COD percentage removal of 59.22% (531mg/L COD measurement). Meanwhile, the green graph bar indicates the presence of Fenton reagents and temperature without visible light which achieves second highest COD percentage removal of 50.00% (651mg/L COD measurement). The purple graph bar represents the presence of Fenton reagents and visible light

without temperature which achieves lower COD percentage removal of 31.41% (893mg/L COD measurement); while the pink graph bar denotes the presence of Fenton reagents without temperature and without visible light which achieves lowest COD percentage removal of 22.81% (1005mg/L COD measurement). The results prove that Photo-Fenton with all the parameters can achieve the best COD removal rate while the presence of light intensity is more important compared with the presence of temperature. The difference in terms of effect size and presence/absence between light intensity and temperature is temperature plays a bigger role in varying range within presence of visible light but the presence of light intensity is the larger contributor in absence/presence conditioning. This phenomenon of comparison is labeled Photo-Fenton and Fenton process where Fenton process is conducted without the presence of visible light. Absence of both temperature and light are significant.

Table 4.6.1: Significance results of temperature and light intensity

Concentration of H_2O_2 (mol/L)	Concentration of $FeSO_4.7H_2O$ (mol/L)	Temperature (^oC)	Light Intensity (Watt)	COD Measurement (mg/L)	COD Removal (mg/L)	COD Percentage Removal (%)
1.0	0.5	35.0	300	531	771	59.22
1.0	0.5	-	300	651	651	50.00
1.0	0.5	35.0	-	893	409	31.41
1.0	0.5	-	-	1005	297	22.81

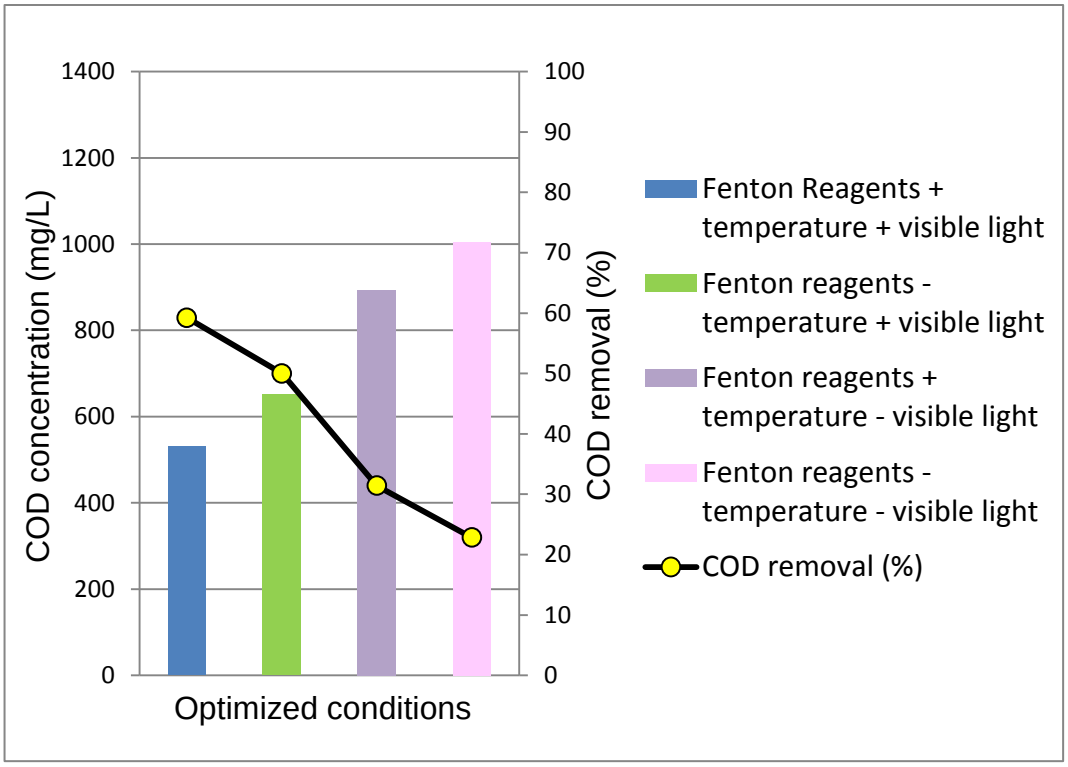

Figure 4.6.1: Significance graph of temperature and light intensity

4.7 Errors In Experimental Procedure

I. **Random error**. DIPA tends to easily absorb water vapour from the surrounding atmosphere. During experimental conduct in preparing standard solution, weight of DIPA solids will then be affected by the presence of water content. Therefore, concentration of the solution will be inaccurate and inconsistent.

II. **Random error**. Constant light irradiation from light source, continuous temperature from hot plate and surrounding temperate atmosphere fluctuates the efficiency and accuracy of experimental setup.

III. **Random error**. 60 minutes of reaction time without any time-interval in between will not show the true degradation rate for Photo-Fenton proces.

IV. **Random error**. Short distance between light source and reaction system causes vaporization to happen which then leads to an increment in concentration as visible light exerts a certain amount of heat.

V. **Systematic error**. COD measurement (mg/L) measured by Hach® DR3900 spectrophotometer is not consistent for the same experimental setup.

VI. **Systematic error**. The experimental setup is restricted due to limitations of apparatus where highly accurate measurement could not be taken.

4.8 Recommendations in Experimental Procedure

I. For better accuracy and consistency, measurement for weight of DIPA solids should be conducted in a fume hood with proper air ventilation. This is to prevent DIPA solids from absorbing water vapour.

II. Better temperature monitoring should be placed into the experimental setup for effective temperature controlling. Black box which fully encompasses the reaction system should be installed to reduce influence from random surrounding fluctuations.

III. Advanced factorial design of experiment should be suggested for calculating other constant parameters instead of just manipulating parameters. More interval in reaction time should be taken for better monitoring control.

IV. Visible light source should be relocated at a calculated distance away from reaction system for prevention of vaporization.

V. Repetition of experiment should be conducted more than three times to reconfirm the accuracy and consistency of the results. Hach® DR3900 spectrophotometer should be calibrated first before usage.

VI. Advanced equipment should be employed for better research results. Laboratory equipments and tools should be calibrated and studied before each usage.

5.0 CONCLUSION

5.1 Overall Conclusion

Photo-Fenton oxidation process utilizes light source with specific chemical products to increase generation rate of •OH radicals. With reference towards reviewing Photo-Fenton oxidation process, the optimization study of DIPA degradation is evaluated using design of experimentation. The objectives of the research are achieved successfully by finding the effect significance of respective parameters and the conditions governing the optimization effect. The four major manipulating parameters are listed as concentration of H_2O_2, concentration of $FeSO_4.7H_2O$, temperature and light intensity; while the three other constant variable are listed as concentration of DIPA (500ppm), pH value (3) and reaction time (60 minutes).

First experimental section explains the blank sample calibration of DIPA in which the value of raw COD measurement is 1302 mg/L. In design of experimentation, the maximum optimization value is achieved by sample run 14 which is 662 mg/L COD removal (50.84% removal) while the lowest optimization value is achieved by sample run 3 which is 32mg/L COD removal (2.46% removal). The conditions for sample run 14 are 1.0M concentration of H_2O_2, 0.1M concentration of $FeSO_4.7H_2O$, temperature at 35^oC and light intensity of 500W while the conditions for sample run 3 are 0.1M concentration of H_2O_2, 1.0M concentration of $FeSO_4.7H_2O$, temperature at 25^oC and light intensity of 300W. The optimization arrangement relating to the order from highest to lowest measurement is calculated to be concentration of H_2O_2 (Factor A), followed by concentration of $FeSO_4.7H_2O$ (Factor B), temperature (Factor C) and finally, light intensity (Factor D). It can be concluded that maximum range should be used for concentration of H_2O_2, temperature and light intensity; while minimum range should be used for concentration of $FeSO_4.7H_2O$.

In accordance to optimization process, the adjusted condition is set at 1.0M concentration of H_2O_2, 0.5M concentration of $FeSO_4.7H_2O$, temperature at 35^oC and light intensity of 300Watt. The specific sample achieved COD measurement of 531mg/L (771 COD removal, 59.22% removal). Through literature review and theories, concentration of H_2O_2 increases the production rate of •OH radicals which

eventually enhances Photo-Fenton process. Besides that, the concentration of $FeSO_4.7H_2O$ is proportionally directed with concentration of H_2O_2 to achieve a certain optimized ratio while temperature at 35^oC acts as a suitable cultivation for production of •OH radicals. These three optimized parameters achieved a value higher than 5% for differences in COD percentage removal between highest range and lowest range. The final parameter consisting of light intensity did not achieve such requirement such as cost to effiency ratio. Therefore, the light intensity is set at 300Watt.

Comparison section explains the significance effect of temperature and light intensity towards Photo-Fenton process. With the presence of both temperature and light intensity, optimization is achieved at highest peak results while the absence of both the parameter could only achieved lowest COD removal rate of 22.81% (297mg/L COD removal, 1005mg/L COD measurement). Presence of light intensity is more significant in comparison with temperature due to the comparison between Photo-Fenton and Fenton process while temperature is just a variable in reaction kinetics. However, optimization process proves that temperature plays a more important role for effect size in varying range of values but the absence/presence of temperature is not literally effective.

Overall, conclusion regarding Photo-Fenton could be drawn in regards for its effective and efficient oxidation process in comparison with Fenton process. The concept of Photo-Fenton in the degradation of DIPA especially among the natural gas department could be useful for future treatment. Main factors considering cost, efficiency and effectiveness could be maximized and capitalized in industrial usage. Finally, the inferences for Photo-Fenton oxidation process could be validated through literature review and theories where similar evidence is proven.

5.2 Relevancy to Objective

In accordance with experimental layout, the efficiency of degradation standard for DIPA can be determined based on several methodology stages. Before the start of experimental analysis, different raw DIPA calibrations have been conducted for COD measurement. Firstly, four major manipulating variables such as concentration of H_2O_2, concentration of $FeSO_4.7H_2O$, temperature and light intensity are being studied through design of experimentation to obtain effect size. Later onwards, each parameter study is evaluated and arranged accordingly from highest to lowest effect size significance. Optimization for the best COD removal rate in Photo-Fenton process is asserted with results which removes more than half the initial COD concentration. The inferences for each Photo-Fenton experimental data is validated through literature review and studies of reaction kinetics. Comparison for significance of temperature and light intensity is the important factor for differences between Photo-Fenton and Fenton processes collaborating with the most important reaction kinetic (temperature). Therefore, the utilization of research project emphasizes on enhancing Photo-Fenton oxidation process as well as to maximize cost to efficiency ratio.

5.3 Recommendation for Future Work

The research project can be extended for further optimization range (higher range and lower range conditioning) for each parameter such as concentration of H_2O_2, concentration of $FeSO_4.7H_2O$, temperature and light intensity. The Photo-Fenton oxidation process can eventually design experimental parameter which includes constant parameter as a varying parameter of study. However, the cost and budget for the equipments and conditioning should be improved for such cases. The application of utilizing higher concentration of DIPA can be implemented for industrial usage. Despite the methodology background, better laboratory equipments and tools would increase the examination standard for Photo-Fenton oxidation process. Moreover, better experimental setup should be conducted in a special and suitable environment. Finally, wider exploration regarding Photo-Fenton process should be conducted on other chemical products to make a comparison for similarity or differences among results.

REFERENCES

AES Arabia Ltd. (2013). Advanced oxidation plants. Retrieved 3rd July, 2014 from http://www.aesarabia.com/advanced-oxidation-plants/

Al-Juaied M. A. (May 2004). Carbon dioxide removal from natural gas by membranes in the presence of heavy hydrocarbons and by Aqueous Diglycolamine®/Morpholine, PhD thesis, pp. 1-424, The University of Texas at Austin, Texas.

Andreozzi R., Caprio V., Insola A. & Marotta R. (1999). Advanced Oxidation Processes (AOPs) for water purification and recovery. Catalyst Today, 53, 51-59.

Binay K. D., Sabtanti Harimurti, Idzham F. M. A., Sampa Chakrabarti & Davide Vione (2010). Degradation of Diethanolamine by Fenton's reagent combined with biological post-treatment. Desalination and Water Treatment 19, 286-293, 1994-3994/ 1994-3986.

Bolton J. R., Bircher K. G., Tumas W. & Tolman C. A. (2001). Figures-of-merit for the technical development and application of Advanced Oxidation Processes. Pure Appl.Chem., v.73, n.4, p.627-637.

Bossmann S. H., Oliveros E., Göb S., Siegwart S., Dahlen E. P. & Payawan Jr. L. (1998). New evidence against hydroxyl radicals as reactive intermediates in the thermal and photochemically enhanced Fenton reactions. J. Phys Chem A. 102(28):5542-50.

Chemspider (2014). Diisopropanolamine. Royal Society of Chemistry, ChemSpider ID: 7624. Retrieved 12th February, 2014 from http://www.chemspider.com/Chemical-Structure.7624.html

Dunn C. L. (1964). Hydrocarbon process. Pet. Refiner, 43, 150.

Durán A., Monteagudo J. M. & Amores E. (2008). Solar Photo-Fenton degradation of Reactive Blue 4 in a CPC reactor. Applied Catalysis B: Environmental 80, 42-50.

European Commission (2007). CO_2 capture and storage projects. Retrieved 3rd July, 2014 from http://ec.europa.eu/research/energy/pdf/synopses_co2_en.pdf

Fisch E. J. (1977). Shell Oil Co. U.S. Pat. 4, 025, 322.

Ghaly M. Y., Härtel G., Mayer R. & Haseneder R. (2001). Photochemical oxidation of p-chlorophenol by UV/H_2O_2 and Photo-Fenton process. A comparative study, Waste Management, v.21, p.41-47.

Glaze W. H., Kang J. W. & Chapin, D. H. (1987). The chemistry of water treatment involving ozone, hydrogen peroxide and ultraviolet radiation. Ozone Science & Engineering, vol 9, no 4, p 335-342.

Goar B. G. & Arrington T. O. (1979). Guidelines set for handling sour gas- part 1 of sour gas treating, sour gas processing and sulfur recovery. Petroleum Publishing.

Gogate P. R. & Pandit A. B. (2004). A review on imperative technologies for wastewater treatment I: oxidation technologies at ambient conditions. Advances in Environmental Research, vol 8, p 501-505.

Hach$_1$ (2004). DRB 200 digester: Dry Thermostat Reactor Data Sheet. Lit 2462. Retrieved 4th July, 2014 from http://www.hach.com/drb200-digital-reactor-block-9-x-16-mm-vial-wells-2-x-20-mm-vial-wells-115-vac/product-downloads?id=7640453261

Hach$_2$ (2010). Hach® DR3900™ UV-VIS spectrometer: DR/3900 Spectrophotometer Data Sheet. Lit 2667. Retrieved 4th July, 2014 from http://www.hachco.ca/dr-3900-benchtop-spectrophotometer-with-rfid-technology/product-downloads?id=14534083396&callback=pf

Hach$_3$ (2014). Hach® DR3900™ UV-VIS spectrometer: Oxygen Demand, Chemical -Reactor Digestion COD Method 8000, TNTPLUS™. Retrieved 4th July, 2014 from http://www.hachco.ca/dr-3900-benchtop-spectrophotometer-with-rfid-technology/product-downloads?id=14534083396&callback=pf

Hazel Mercantile Limited (2007). Di-isopropanolamine – Material Safety Data Sheet. Retrieved 14th February, 2014 from http://hmlindia.com/MSDS/Diisopropanolamine.pdf

Huang C. P., Dong C. & Tang Z. (1993). Advanced chemical oxidation: its present role and potential future in hazardous waste treatment. – Waste Management, vol 13, p 361-377.

Hullu J. D., Maassen J. I. W., Van Meel P. A., Shazad S., Vaessen J. M. P., Bini L. & Reijenga J. C. (2008). Comparing different biogas upgrading techniques. Interim Report, Dirkse Milieutechniek, Eindhoven University of Technology.

Huston P. L. & Pignatello J. J. (1999). Degradation of selected pesticide active ingredients and commercial formulations in water by the photoassisted Fenton reaction. Water Research, Vol. 32, No. 2, pp. 489-497, ISSN 0043-1354.

Hwang, Yun Whan Kang & Kyung-Yub (2000). Effects of reaction conditions on the oxidation efficiency in the Fenton process. Wat. Res., 34(10), 2786-2790.

Jordi Bacardit, Isabel Oller, Manuel I. Maldonado, Ester Chamarro, Sixto Malato & Santiago Esplugas (2007). Simple Models for the Control of Photo-Fenton by Monitoring H_2O_2. J. Adv. Oxid. Technol, 10(2), 219-228.

Kim, Vogelpohl A. & S. M. (2004). Advanced Oxidation Processes (AOPs) in wastewater treatment. Ind. Eng. Chem, 10(No.1), 33-40.

Klemes J., Bulatov I. & Cockerill T. (2005). Techno-economic modeling and cost functions of CO_2 capture processes. Comput, Aided Chem. Eng., 20, 295-300.

Kochany J. & Bolton J. R. (1992). Mechanism of photodegradation of aqueous organic pollutants. 2. Measurement of the primary rate constants for reaction of OH radicals with benzene and some halobenzens using an EPR spin-trapping method following the photolysis of H_2O_2 – Environmental Science and Technology, vol 26, p 262-265.

Kohl A. L. & Nielsen R. B. (1997). Gas Purification (5th edition), Gulf Professional Publishing, ISBN 978-0-8841-5220-0, Texas.

MacGregor R. J. & Mather A. E. (1991). Can. J. Chem. Eng., 69, 1357-1366.

Mckinsey Zicari S. (2003). Removal of hydrogen sulfide from biogas using cow-maure compost. Thesis (M.S.)- Cornell University, Jan 2003.

Montserrant Pèrez, Francesc Torrandes, Xavier Domènech & Jose Peral (2002). Fenton and Photo-Fenton oxidation of textile effluents. Water Research, 36, 2703-2710.

Moraes J. E. F., Quina F. H., Nascimento C. A. O., Silva D. N. & Chiavone-Filho O. (2004). Treatment of saline wastewater contaminated with hydrocarbons by the Photo-Fenton process. Environ Sci Technol 2004(a); 38 (4): 1183-7.

Moraes J. E. F., Silva D. N., Quina F. H., Chiavone-Filho O. & Nascimento C. A. O. (2004). Utilization of solar energy in the photodegradation of gasoline in water and of oil-field-produced water. Environ Sci Technol 2004(b); 38(4): 3746-51.

Murrieta-Guevarra & et al. (1994). Fluid Phase Equilib., 95, 163-174.

Ollis D. (1993). Comparative aspects of advanced oxidation processes. Emerging Technologies in Waste Management II, ACS Symposium Series 518. Washington, DC, p. 18-34.

Oppenländer T. (2003). Advanced Oxidation Processes (AOPs): Principles, reaction mechanisms, reactor concepts: Wiley VCH, Weinheim. ISBN 3-527-30563-7.

Pascoli S. D., Femia A. & et al. (2001). Natural gas, cars and the environment. A (relatively) ‘clean’ and cheap fuel looking for users. Ecological Economics, Vol. 38, No.2, pp.179-189.

Pera-Titus M., García-Molina V., Baños M. A., Giménez J. & Esplugas S. (2004). Degradation of chlorophenols by means of Advanced Oxidation Processes: A general review. Applied Catalysis B: Environmental, v.47, p.219-256.

Pérez-Moya M., Graells M., Delvalle L. J., Centelles E. & Mansilla H. D. (2007). Fenton and Photo-Fenton degradation of 2-chlorophenol: Multivariate analysis and toxicity monitoring. Catalysis Today, v.124, p.163-171.

Pignatello J. J. (1992). Dark and photoassisted iron (3+)-catalyzed degradation of chlorophenoxy herbicides by hydrogen peroxide. Environ Sci Technol; 26(5): 944-51.

Ritchie L. L. Z. (2013). Efficiency of Diisopropanolamine (DIPA) degradation with different visible light intensitities under Photo-Fenton Oxidation. Project Dissertation: Universiti Teknologi PETRONAS.

Ritter, J. A. and Ebner A. D. (2007). Carbon Dioxide Separation Technology: R&D Needs for the Chemical and Petrochemical Industries, In: Recommendation for future R&D, 22.06.11. Available from: http://www.chemicalvision 2020.org/pdfs/CO2_Separation_Report_V2020_final.pdf

Ruppert G., Bauer R. & Heisler, G. (1993). The Photo-Fenton reaction – An effective photochemical wastewater treatment process. Journal of Photochemistry and Photobiology A: Chemistry, Vol. 73, No. 1, pp. 75-78, ISSN 1010-6030.

Ryckebosch E., Drouillon M. & Vervaeren H. (2011). Techniques for transformation of biogas to biomethane. Journal of Biomass and Bioenergy 35 1633-1645.

Sabtanti Harimurti, Abul Aziz Omar, Anisa Ur Rahmah & Thanpalan Murugesan (2011). The degradation mechanism of Wastewater Containing MDEA using UV/H_2O_2 Advanced Oxidation Process. 978-1-4577-1884-7/11/$26.00©2011 IEE.

Safarzadeh-Amiri A., Bolton J. R. & Cater S. R. (1997). Ferrioxalate-mediated photodegradation of organic pollutants in contaminated water. Water Research, v.31, n.4, p.787-798.

Siemens (2011). Tertiary Wastewater Treatment. Retrieved 17th February, 2014 from http://www.water.siemens.com/en/applications/wastewater_treatment/ metals-removal/Pages/default.aspx

Simmonds M., Hurst P., Wilkingson M. B., Watt C. & Roberts C. A. (2002). A study of very large scale post combustions CO_2 capture at a refining & petrochemical complex. Proc. 6th Int. Conf. on Greenhouse Gas Control Technologies, Kyoto 39-44.

Sorensen J. A., Fraley R. H., Gallagher J. R. & Schmit C. R. (1996). Background report on subsurface environmental issues relating to natural gas sweetening and dehydration operations. Gas Research Institute, Technical Report, March, 1996.

Stasinakis A. S. (2008). Use of selected advanced oxidation processes (AOPs) for Wastewater Treatment – A mini Review. Global NEST Journal, 10 (3), 376 -385.

Thomas C. (2012). Overview of heat exchanges for amine gas treating application. Hydrocarbon Engineering: Tranter International AB, Sweden, 2012. Available from http://www.tranter.com/literature/markets/hydrocarbon-processing/Hydrocarbon-Eng-A-Sweet-Treat.pdf

Ullmann's (1991). Encyclopaedia of industrial chemistry. Germany: VCH Verladsgesellschaft, 5th ed., p 415-419.

U.S. EIA (2010). International energy outlook 2010. Washington, DC. Retrieved 5th July, 2014 from http://www.eia.doe.gov/oiaf/ieo

Will I. B. S., Moraes J. E. F., Teixeira A. C. S. C., Guardani R. & Nasimento C. A. O. (2004). Photo-Fenton degradation of wastewater containing organic compounds. Sep Purif Technol; 34:51-7.

Yang Hongjun, Fan Shuanshi, Lang Xuemei, Wang Yanhong & Nie Jianghua (2011). Economic comparison of three gas separation technologies for CO_2 capture from power plant flue gas. Separation Science and Engineering- Chinese Journal of Chemical Engineering, 19(4), 615-620.

Yogish K. (1990). Can. J. Chem. Eng., 68, 511-512.

Youssef S., Emna H. & Ridha A. (2012). Fenton and solar Photo-Fenton processes for the removal of chlorpyrifos insecticide in wastewater. ISSN0378-4738. Available from: http://dx.doi.org/10.4314/wsa.v38i4.8

Zhang A. L. & Fang D. (1996). Greenhouse gas CO_2 control and recovery, China environmental science press, Beijing.

Appendix A: Specifications of Hach DRB 200 Digestor (Hach$_1$, 2004)

DATA SHEET

DRB 200 Dry Thermostat Reactor

Digestion

Features and Benefits

Easy to Use and Fast

The Hach DRB 200 Dry Thermostat Reactor provides unique one-key operation. Programs for Hach procedures with digestion are preprogrammed into the instrument. And it's fast—the block heats from 20 to 150°C in less than 10 minutes.

Safe to Operate

The fully insulated heater block of the DRB 200 reactor means there can be no skin contact with the heater block. Temperature safeguards are provided to prevent overheating. The lids are transparent and lock do deter premature checking of the progress of the reaction. And the reactor will emit an audible signal and automatically shutdown at the end of the run.

Versatile

Use the DRB 200 reactor for digestions for metals analysis, digestions for nutrients analysis, or culture biological samples. Control temperatures in the reactor from 37 to 165°C in 1°C increments. In addition to preprogrammed digestion methods, use the reactor to program and store up to three custom methods.

Accommodates Most Test Vials

The DRB 200 reactor can heat solutions in round vials of two different sizes. Small, 16-mm diameter vial wells are suitable for Hach COD, UniCel™, TOC, and Test 'N Tube vials. Larger, 20-mm diameter vial wells are intended for sample preparation reaction vessels using the Metals Prep Set.

Hach's DRB 200 Dry Thermostat Reactor is the simple solution for standard and special digestions. It is preprogrammed for all standard digestions and can be user programmed for other digestions. Excellent reproducibility is assured because of its temperature stability. One-key operation for standard digestions makes it easy to use.

DW WW PW IW E FB

Optional Dual Block for Simultaneous Digestions

Two heat blocks in the DRB200 reactor give the operator independent control of two temperatures and durations. Use this option to run two programs at the same time.

Applications

	Temperature (°C)	Time (minutes)
COD	150	120
TOC	105	120
ISO-TOC		
Metals, suspended and/or complexed (lead, cadmium, copper, iron, nickel, zinc)	100	60
Total Chromium	100	60
Total Nitrogen	100/105*	60/30
Total Phosphate	100/105*	60/30
Trihalogenmethane	100	8
User-specific programs	37 to 165	1 to 480

*Digestion temperature and time depend on test method and reagents selected.

DW = drinking water WW = wastewater municipal PW = pure water / power
IW = industrial water E = environmental C = collections FB = food and beverage

HACH®

Be Right™

Specifications*

Programmable Temperature Range
37 to 165°C (99 to 329°F)

Operating Temperature
10 to 45 °C (50 to 113°F)

Programmable Timer Range
0 to 480 minutes

Heating Rate
20 to 150°C in 10 minutes

Temperature Stability
± 1°C

Stored Programs

COD	150°C	120 minutes
TOC	105°C	120 minutes
Fixed	100, 105, 150, 165°C	30, 60, 120 minutes

Power Requirements
100 to 240 Vac, 50/60 Hz, 600 VA

Compliance
CE, GS, cTUVus

Dimensions
25.0 x 14.5 x 31.0 cm
(9.8 x 5.7 x 12.2 in.)

Number of Vial Wells
Single block:
9 16-mm and 2 20-mm or 15 16-mm

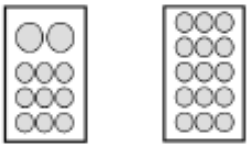

Dual block:
21 16-mm and 4 20-mm

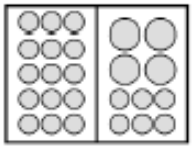

Weight
Single block: 2 kg (4.4 lbs.)
Dual block: 2.8 kg (6.2 lbs.)

Warranty
Two-year

*Specifications subject to change without notice.

Engineering Specifications

1. The digestion reactor shall be a bench top instrument for heating prepared samples to temperature for the designated time for the test.
2. The instrument shall have a programmable temperature range of 37 to 165°C.
3. The instrument shall have a programmable timer range of 0 to 480 minutes.
4. The instrument shall have a heating rate of 20 to 150°C in 10 minutes.
5. The instrument shall be equipped with stored digestion programs.
   a. COD: 150°C; 120 minutes
   b. TOC: 105°C; 120 minutes
   c. Fixed: 100, 105, 150, 165°C; 30, 60, 120 minutes
6. The instrument shall accommodate 16-mm and or 20-mm vials.
7. The power requirements of the instrument shall be 100-240 Vac, 50/60 Hz.
8. The instrument shall be Model DRB 200 Dry Thermostat Reactor manufactured by Hach Company.

Ordering Information

LTV082.53.30001	DRB 200-1, single block, 9 16-mm and 2 20-mm vial wells
LTV082.53.40001	DRB 200-1, single block, 15 16-mm vial wells
LTV082.53.42001	DRB 200-2, dual block, 21 16-mm and 4 20-mm vial wells

Lit. No. 2462
XXXX Printed in U.S.A.

At Hach, it's about learning from our customers and providing the right answers. It's more than ensuring the quality of water—it's about ensuring the quality of life. When it comes to the things that touch our lives...

Keep it pure.

Make it simple.

Be right.

For current price information, technical support, and ordering assistance, contact the Hach office or distributor serving your area.

In the United States, contact:

HACH COMPANY World Headquarters
P.O. Box 389
Loveland, Colorado 80539-0389
U.S.A.
Telephone: 800-227-4224
Fax: 970-669-2932
E-mail: orders@hach.com
www.hach.com

U.S. exporters and customers in Canada, Latin America, sub-Saharan Africa, Asia, and Australia/New Zealand, contact:

HACH COMPANY World Headquarters
P.O. Box 389
Loveland, Colorado 80539-0389
U.S.A.
Telephone: 970-669-3050
Fax: 970-461-3939
E-mail: intl@hach.com
www.hach.com

In Europe, the Middle East, and Mediterranean Africa, contact:

HACH + LANGE Europe
Dr. Bruno Lange GmbH & Co. KG
Willstätterstraße 11
D-40549 Düsseldorf
GERMANY
Tel: +49 (0) 211 5288-0
Fax: +49 (0) 211 5288-143
E-mail: kundenservice@drlange.de
www.drlange.com

HACH®
Be Right™

Appendix B: Specifications of Hach® DR3900 Spectrophotometer (Hach$_2$, 2010)

DR 3900™ SPECTROPHOTOMETER

Applications
- Beverage
- Drinking Water
- Wastewater
- Food QC Lab
- Power

Prevent measurement errors...simply.

The proven technology you have come to expect from Hach just got better. Built with the future of water analysis in mind, the DR 3900 will give consistently accurate results in a simpler testing format.

Guided Procedure

The DR 3900 guides you step-by-step through the testing procedure like a GPS, so you can get the accurate results you need every time.

Elimination of False Readings

Scratched, flawed, or dirty glassware becomes a non-issue when your machine takes 10 readings and eliminates outliers.

Hands Free Updates*

RFID technology automatically updates the program calibration factors when you place a TNTplus box near the machine.

Flexible Connectivity

Built with 1 ethernet and 3 USB ports, the DR 3900 easily connects to your computer and is programmed to easily interface with Hach WIMS™ or any LIMS system.

Sample Tracking*

Sample bottles with smart tags can easily be tracked with the optional Hach RFID sample-ID system, eliminating sample mix-ups and providing better sample traceability.

*RFID technology currently available only in US, Anguilla, American Samoa, Australia, Bolivia, Canada, Cayman Islands, Columbia, Dominican Republic, El Salvador, Federated States of Micronesia, Guam, Guatemala, Marshall Islands, New Zealand, Northern Mariana Islands, Palau, Panama, Puerto Rico, and US Virgin Islands.

HACH®
Be Right™

Specifications*

Operating Mode	Transmittance (%), Absorbance and Concentration, Scanning
Light Source	Gas-filled Tungsten (visible)
Optical System	Reference beam, spectral
Wavelength Range	320 to 1100 nm
Wavelength Accuracy	± 1.5 nm (wavelength range 340 to 900 nm)
Wavelength Reproducibility	± 0.1 nm
Wavelength Resolution	1 nm
Wavelength Calibration	Automatic
Wavelength Selection	Automatic, based on method selection
Spectral Bandwidth	5 nm
Photometric Measuring Range	± 3.0 Abs (wavelength range 340 to 900 nm)
Photometric Accuracy	5 mAbs at 0.0 to 0.5 Abs 1 % at 0.50 to 2.0 Abs
Photometric Linearity	< 0.5 % to 2 Abs ≤ 0.01 % at >2 Abs with neutral glass at 546 nm
Stray Light	< 0.1 % T at 340 nm with $NaNO_2$
Display	7 TFT WVGA (800 pix x 480 pix)

Data Logger	2000 measured values (Result, Date, Time, Sample ID, User ID)
Preprogrammed Methods	> 240
User Programs	100
Sample Cell Compatibility	13 mm round, 16 mm round, 1 cm & 5 cm rectangular, 1 round, 1 square
Dimensions (H x W x D)	5.9 in x 13.8 in x 10 in (151 mm x 350 mm x 255 mm)
Weight	9.26 lbs. (4.2 kg)
Operating Conditions	10 to 40 °C
Storage Conditions	-30 to 60 °C
Enclosure Rating	IP30
Power Supply	Benchtop Power Supply
Power Requirements (Voltage)	110 - 240 V AC
Power Requirements (Hz)	50/60 Hz
Interfaces	USB type A (2), USB type B, Ethernet, RFID module
Warranty	12 months

*Subject to change without notice.

Principle of Operation

Hach's TNTplus chemistries and spectrophotometers are made to work seamlessly with each other.

- *Many of the tests are EPA compliant.*
- *Over 35 tests available including these popular EPA Approved Parameters:*
  - *Ammonia*
  - *COD*
  - *Chlorine*
  - *Chromium*
  - *Iron*
  - *Nitrate*
  - *Nitrite*
  - *Nitrogen*
  - *Phosphorus*
  - *Sulfate*

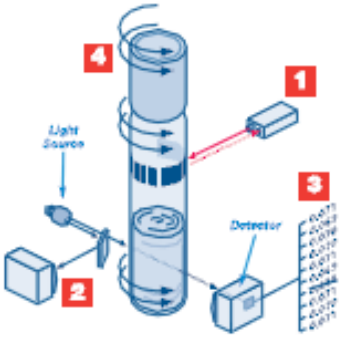

How TNTplus Works

1 Barcode Recognition
Simply drop in the vial and get results immediately with automatic method detection.

2 Reference Detector
Monitors and compensates for optical fluctuations.

3 10X Measurement and Outlier Elimination
Dirty, scratched, or fingerprinted glassware, including fingerprints, is no longer an issue—instrument averages 10 readings and rejects outliers.

4 Self-Contained Packaging—Reagents Inside Sealed Cap
Reduces exposure to chemicals—no need to open pillows or clean glassware.

See our TNTplus video at: www.hach.com/tnplus

hach.com

Available Tests

The following table lists available tests and overall ranges for the Hach DR 3900 Benchtop Spectrophotometer. The ranges may represent more than one available test for the instrument. Consult your Hach representative, Customer Service, the Hach Master Catalog, or the Hach web site at www.hach.com for complete details of all available tests for this instrument.

Parameter	Range	TNTplus Test
Alachlor	0.1 to 0.5 ppb, threshold	
Alkalinity, Total	25 to 400 mg/L	•
Aluminum	0.002 to 0.800 mg/L	•
Ammonia, Nitrogen	0.015 to 50.0 mg/L	•
Arsenic	0.020 to 0.200 mg/L	
Atrazine	0.5 to 3.0 ppb, threshold	
Barium	2 to 100 mg/L	
Benzotriazole	1.0 to 16.0 mg/L	
Boron	0.2 to 14.0 mg/L	
Bromine	0.05 to 4.50 mg/L	
Cadmium	.7 µg/L to 0.30 mg/L	•
Carbohydrazide	5 to 600 µg/L	
Chloramine, Mono	0.04 to 10.0 mg/L	
Chloride	0.1 to 25.0 mg/L	
Chlorine Dioxide	0.01 to 1000 mg/L	
Chlorine, Free	0.02 to 10.0 mg/L	•
Chlorine, Total	2 µg/L to 10.0 mg/L	•
Chromium, Hexavalent	0.010 to 1.00 mg/L	•
Chromium, Total	0.01 to 0.70 mg/L	•
Cobalt	0.01 to 2.00 mg/L	
Color	3 to 500 units	
COD (Chemical Oxygen Demand)	0.7 to 15,000 mg/L	•
Copper	1 µg/L to 8.0 mg/L	•
Cyanide	0.002 to 0.240 mg/L	
Cyanuric Acid	5 to 50 mg/L	
DEHA (Diethylhydroxylamine)	3 to 450 µg/L	
Dissolved Oxygen	6 µg/L to 40 mg/L	
Erythorbic Acid (Isoascorbic acid)	13 to 1500 µg/L	
Fluoride	0.02 to 2.00 mg/L	
Formaldehyde	3 to 500 µg/L	
Hardness, Total (Calcium and Magnesium as $CaCO_3$)	4 µg/L to 4.00 mg/L	
Hydrazine	4 to 600 µg/L	
Hydroquinone	9 to 1000 µg/L	
Iodine	0.07 to 7.00 mg/L	
Iron, Ferrous	0.02 to 3.00 mg/L	
Iron, Total	0.009 to 6.0 mg/L	•

Parameter	Range	TNTplus Test
Lead	3 µg/L to 2.0 mg/L	•
Manganese	0.006 to 20.0 mg/L	
Mercury	0.1 to 2.5 µg/L	
Methylethylketoxime (MEKO)	15 to 1000 µg/L	
Molybdenum, Molybdate	0.02 to 40.0 mg/L	
Nickel	0.006 to 6.0 mg/L	•
Nitrate, Nitrogen	0.01 to 35 mg/L	•
Nitrite, Nitrogen	0.002 to 250 mg/L	•
Nitrogen, Simplified Total Kjeldahl	0 to 16 mg/L	•
Nitrogen, Total	0.5 to 150 mg/L	•
Nitrogen, Total Inorganic	0.2 to 25.0 mg/L	
Nitrogen, Total Kjeldahl	1 to 150 mg/L	
Ozone	0.01 to 1.50 mg/L	
PCB (Polychlorinated Biphenyls)	1 to 50 ppm, threshold	
Phenols	0.002 to 0.200 mg/L	
Phosphonates	0.02 to 125.0 mg/L	
Phosphorus, Acid Hydrolyzable	0.06 to 100.0 mg/L	
Phosphorus, Reactive (Orthophosphate)	19 µg/L to 100.0 mg/L	•
Phosphorus, Total	0.06 to 100.0 mg/L	•
Potassium	0.1 to 7.0 mg/L	
Quaternary Ammonium Compounds	0.2 to 5.0 mg/L	
Selenium	0.01 to 1.00 mg/L	
Silica	3 µg/L to 100 mg/L	
Silver	0.005 to 0.700 mg/L	
Sulfate	2 to 900 mg/L	•
Sulfide	5 to 800 µg/L	
Surfactants, Anionic	0.002 to 0.275 mg/L	
Suspended Solids	5 to 750 mg/L	
Tannin and Lignin	0.1 to 9.0 mg/L	
TOC (Total Organic Carbon)	0.3 to 700 mg/L	
Tolyltriazole	1.0 to 20.0 mg/L	
Toxicity	0 to 100% Inhibition	
TTHM (Trihalomethanes, Total)	10 to 600 µg/L	
TPH (Total Petroleum Hydrocarbons)	2 to 200 ppm, threshold	
Volatile Acids	27 to 2800 mg/L	•
Zinc	0.01 to 3.00 mg/L	

Ordering Information

DR5000-03 DR 5000 UV-Vis Spectrophotometer, 100-240 Vac; includes multi-cell holder, instrument manual, power cords (115V and 230V), 1-in. matched glass sample cells, 1 cm matched quartz sample cells

Optional Accessories

LZV478 Carousal Sample Changer; holds up to seven 1 cm square sample cells

LZV485 Sipper Module; includes 1 cm square quartz cell

LZV479 Pour-Thru Cell Kit, 1-in.

LZV789 Pour-Thru Cell Kit, 1 cm

LZY421 Cell Adapter for 10 cm x 1 cm rectangular cells

LZY274 DataTrans™ Software
Hach DataTrans Software transfers measurement output from Hach DR 2700, DR 2800, or DR 5000 spectrophotometers to a PC via USB port. This direct computer file input saves time and eliminates keying errors. Data can be transferred to an Excel spreadsheet or to LIMS. The software also displays wavelength scan and time course graphs, and underlying raw data points can be easily exported to Excel. A powerful search function allows customer to sort by: Result (parameter), Date (range), Operator, Instrument (type, serial number), Program (name, type), and Sample name. For recurring searches, users may also create custom search programs and save under separate names.

LZV669 Brewery Analysis Package
The Brewery Analysis Software package is designed for breweries utilizing the Hach DR 5000 Spectrophotometer. This upgrade contains 12 specific brewery assays that conveniently upload via USB to a DR 5000. Assays are based on published and observed brewing methods and include procedures for: • Anthocyanogens • Iron • Steam volatile phenols • Beer color • Iso-alpha-acids • Total polyphenols • Bitterness units • Photometric iodine • Thiobarbituric acid number (TAN) • Free amino nitrogen • Reductones • Vicinal diketones

LZV537 Certified Test Filter Set
Consists of six filters for checking the absorbance accuracy, stray light, and wavelength accuracy. Designed for use with the standard 10mm cell holder. The set is supplied in a sturdy wooden case. For identification purposes, the filter name, set number and part number are printed on each filter mount. The absorbance values and/or peak position wavelengths of each filter are quoted in the accompanying calibration certificate.

2960100 Citizen PD-24 Printer Package
Includes printer, universal power supply, 115V power cord, battery pack, USB cable, RS232 cable with gender adapter, and one roll of thermal paper.

To complete your laboratory analytical instrumentation, choose from these new chemistries...

TNTplus™ Reagent Vials

Hach TNTplus reagent vials are bar-coded for automatic method detection when used with the DR 5000 Spectrophotometer to save time, minimize errors, and reduce laboratory costs. 10-fold measurement and rejection of outliers allows for improved accuracy and precision. (Complete list of available parameters on page 3.)

Lit. No. 2479 Rev 4
H10 Printed in U.S.A.

At Hach, it's about learning from our customers and providing the right answers. It's more than ensuring the quality of water—it's about ensuring the quality of life. When it comes to the things that touch our lives...

Keep it pure.

Make it simple.

Be right.

For current price information, technical support, and ordering assistance, contact the Hach office or distributor serving your area.

In the United States, contact:

HACH COMPANY World Headquarters
P.O. Box 389
Loveland, Colorado 80539-0389
U.S.A.
Telephone: 800-227-4224
Fax: 970-669-2932
E-mail: orders@hach.com
www.hach.com

U.S. exporters and customers in Canada, Latin America, sub-Saharan Africa, Asia, and Australia/New Zealand, contact:

HACH COMPANY World Headquarters
P.O. Box 389
Loveland, Colorado 80539-0389
U.S.A.
Telephone: 970-669-3050
Fax: 970-461-3939
E-mail: intl@hach.com
www.hach.com

In Europe, the Middle East, and Mediterranean Africa, contact:

HACH LANGE GmbH
Willstätterstraße 11
D-40549 Düsseldorf
GERMANY
Tel: +49 (0) 211 5288-0
Fax: +49 (0) 211 5288-143
E-mail: info@hach-lange.de
www.hach-lange.com

HACH®
Be Right™

Appendix C: User Manual of Hach® DR3900 Spectrophotometer (Hach$_3$, 2014)

Oxygen Demand, Chemical

DOC316.53.01100

USEPA[1] Reactor Digestion Method[2] — **Method 8000**

3 to 150 mg/L COD (LR) — **TNTplus™ 821/822**

20 to 1500 mg/L COD (HR)

Scope and application: For water, wastewater; digestion is required.

[1] COD ranges 3–150 mg/L and 20– 1500 mg/L COD are USEPA approved (5220 D) for wastewater analyses, Federal Register, April 21, 1980, 45(78), 26811-26812

[2] Jirka, A.M.; Carter, M.J., Analytical Chemistry, 1975, 47(8), 1397

Test preparation

Instrument-specific information

Table 1 shows all of the instruments that have the program for this test. The table also shows the adapter and light shield requirements for the applicable instruments that can use TNTplus vials.

To use the table, select an instrument, then read across to find the applicable information for this test.

Table 1 Instrument-specific information for TNTplus vials

Instrument	Adapters	Light shield
DR 6000, DR 5000	—	—
DR 3900	—	LZV849
DR 3800, DR 2800	—	LZV546
DR 1900	9609900 or 9609800 (A)	—

Before starting

DR 3900, DR 3800, DR 2800: Install the light shield in Cell Compartment #2 before this test is started.
Review the safety information and the expiration date on the package.
The recommended temperature for samples and reagents is 15–25 °C (59–77 °F).
The recommended temperature for reagent storage is 15–25 °C (59–77 °F).
The reagent that is used in this test is corrosive and toxic. Use protection for eyes and skin and be prepared to flush any spills with running water.
Spilled reagent will affect test accuracy and is hazardous to skin and other materials. Be prepared to wash spills with running water.
The reagents that are used in this test contain mercury. Collect the reacted samples for proper disposal.
Run one blank with each set of samples. Refer to Blanks for colorimetric determination on page 3. Run all tests (the samples and the blank) with the same lot of vials. The lot number is on the container label.
Keep unused (light sensitive) vials in a closed box.
Use the DRB reactor with 13-mm wells for the digestion. If the reactor has 16-mm wells, insert adapter sleeves into the wells.
DR 1900: Go to All Programs>LCK or TNTplus Methods>Options to select the TNTplus number for the test. Other instruments automatically select the method from the barcode on the vial.
Review the Safety Data Sheets (MSDS/SDS) for the chemicals that are used. Use the recommended personal protective equipment.
Dispose of reacted solutions according to local, state and federal regulations. Refer to the Safety Data Sheets for disposal information for unused reagents. Refer to the environmental, health and safety staff for your facility and/or local regulatory agencies for further disposal information.

Items to collect

Description	Quantity
COD TNTplus™ Reagent Set, LR or HR	1
DRB200 reactor with 13-mm wells	1
Blender, 2-speed	1
Pipet, adjustable volume, 1.0–5.0 mL	1
Pipet tips, for 1.0–5.0 mL pipet	1
Test tube rack	1

Refer to Consumables and replacement items on page 5 for order information.

Sample collection and storage

- Collect samples in clean glass bottles. Use plastic bottles only if they are known to be free of organic contamination.
- Test biologically active samples as soon as possible.
- Homogenize samples that contain solids to get a representative sample.
- To preserve samples for later analysis, adjust the sample pH to less than 2 with concentrated sulfuric acid (approximately 2 mL per liter). No acid addition is necessary if the sample is tested immediately.
- Keep the preserved samples at 2–6 °C (36–43 °F) for a maximum of 28 days.
- Correct the test result for the dilution caused by the volume additions.

Test procedure

1. Set the DRB200 reactor power to on. Set the temperature to 150 °C.

2. Measure 100 mL of sample in a blender. Blend for 30 seconds or until homogenized.
If the sample does not have suspended solids, ignore this step.

3. Pour the homogenized sample into a 250-mL beaker and stir slowly with a magnetic stir plate.
If the sample does not have suspended solids, ignore this step.

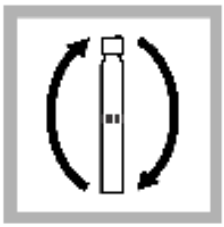

4. Invert a test vial several times to mix.

6. Use a pipet to add 2.0 mL of sample to the test vial.

8. Hold the vial by the cap, over a sink. Invert gently several times to mix. **The vial gets very hot during mixing.**

7. Insert the vial in the preheated DRB200 reactor. Close the lid.

8. Keep the vial in the reactor for 2 hours.

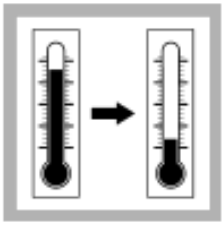

9. When the timer expires, set the reactor power to off. Let the temperature decrease for about 20 minutes to 120 °C or less.

10. Hold the vial by the cap and invert gently several times while the vial is still hot.

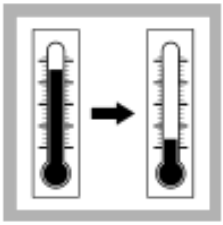

11. Put the vial in a test tube rack. Let the temperature of the vial decrease to room temperature.

12. Clean the vial.

13. DR 1900 only: Select program 821 (LR) or 822 (HR). Refer to Before starting on page 1.

14. Insert the vial into the cell holder. DR 1900 only: Push READ. Results show in mg/L COD.

Blanks for colorimetric determination

Replace the sample with deionized water in the test procedure to determine the reagent blank value. Subtract the reagent blank value from the sample results automatically with the reagent blank adjust option. Use the blank again for other measurements with the same lot of vials. For storage, keep the blanks in a dark location. Monitor the decomposition of the blanks by periodically measuring its concentration. Measure the reagent blank value when a new lot of reagent is used.

To subtract the value of the blanks from a series of measurements:

1. Replace the sample with deionized water in the test procedure to determine the reagent blank value. Clean the vial, then put it in the cell holder. Close the lid.
2. Set the reagent blank function to on. The measured value of the reagent blank is shown.

   Note: *As an alternative, record or enter the reagent blank value at a different time. Push the highlighted reagent blank box and use the keypad to enter the value.*

Interferences

Chloride is the primary interference in this test method and results in a positive interference. Each COD vial contains mercuric sulfate that will eliminate chloride interference to a maximum of 2000 mg/L Cl^-.

Accuracy check

Standard solution method—LR

Use the standard solution method to validate the test procedure, the reagents and the instrument.

Items to collect:

- COD Standard Solution, 1000-mg/L COD
- 100-mL volumetric flask, Class A
- 10.0-mL volumetric pipet, Class A and pipet filler safety bulb
- Deionized water

1. Prepare a 100-mg/L COD standard solution as follows:
   a. Use a pipet to add 10.0 mL of a 1000-mg/L COD standard solution into the volumetric flask.
   b. Dilute to the mark with deionized water. Mix well. Prepare this solution daily.
2. Use the test procedure to measure the concentration of the prepared standard solution.
3. Compare the expected result to the actual result.

   Note: *The factory calibration can be adjusted slightly with the standard adjust option so that the instrument shows the expected value of the standard solution. The adjusted calibration is then used for all test results. This adjustment can increase the test accuracy when there are slight variations in the reagents or instruments.*

Standard solution method—HR

Use the standard solution method to validate the test procedure, the reagents and the instrument.

Items to collect:

- COD Standard Solution, 300-mg/L, 800-mg/L or 1000-mg/L COD or Oxygen Demand Standard (contains 617-mg/L COD) or Wastewater Influent Standard Solution, Mixed Parameter (contains 500-mg/L COD)

1. Use the test procedure to measure the concentration of the standard solution.
2. Compare the expected result to the actual result.

   Note: *The factory calibration can be adjusted slightly with the standard adjust option so that the instrument shows the expected value of the standard solution. The adjusted calibration is then used for all test results. This adjustment can increase the test accuracy when there are slight variations in the reagents or instruments.*

Method performance

The method performance data that follows was derived from laboratory tests that were measured on a spectrophotometer during ideal test conditions. Users can get different results under different test conditions.

Program	Standard	Precision (95% Confidence Interval)	Sensitivity Concentration change per 0.010 Abs change
barcode (TNTplus 821, LR)	75 mg/L COD	72–78 mg/L COD	—
barcode (TNTplus 822, HR)	750 mg/L COD	736–764 mg/L COD	—

Summary of Method

The mg/L COD results are defined as the mg of O_2 consumed per liter of sample under conditions of this procedure. In this procedure, the sample is heated for 2 hours with a strong oxidizing agent, potassium dichromate. Oxidizable organic compounds react, reducing the dichromate ion ($Cr_2O_7^{2-}$) to green chromic ion (Cr^{3+}). With this method, the amount of yellow Cr^{6+} that remains is determined. The COD reagent also contains silver and mercury ions. Silver is a catalyst, and mercury is used to complex chloride interferences. The measurement wavelength is 420 nm for the LR or 620 nm for the HR.

Consumables and replacement items

Required reagents

Description	Quantity/Test	Unit	Item no.
COD TNTplus™ Reagent Set, LR, 3 to 150 mg/L COD	1–2 vials	25/pkg	TNT821
COD TNTplus™ Reagent Set, HR, 20 to 1500 mg/L COD	1–2 vials	25/pkg	TNT822

Required apparatus

Description	Quantity/test	Unit	Item no.
Blender, 2-speed, 120 VAC option	1	each	2616100
Blender, 2-speed, 240 VAC option	1	each	2616102
DRB 200 Reactor, 115 VAC option, 9 x 13 mm + 2 x 20 mm, 1 block	1	each	DRB20001
DRB 200 Reactor, 230 VAC option, 9 x 13 mm + 2 x 20 mm, 1 block	1	each	DRB20005
Pipet, adjustable volume, 1.0–5.0 mL	1	each	BBP065
Pipet tips, for 1.0–5.0 mL pipet	1	75/pkg	BBP068
Light shield, DR 3800, DR 2800, DR 2700	1	each	LZV646
Light shield, DR 3900	1	each	LZV849

Recommended standards

Description	Unit	Item no.
COD Standard Solution, 300-mg/L	200 mL	1218629
COD Standard Solution, 800-mg/L	200 mL	2672629
COD Standard Solution, 1000-mg/L	200 mL	2253929
Oxygen Demand Standard (BOD, COD, TOC), 10-mL ampules	16/pkg	2833510
Wastewater Effluent Standard Solution, Mixed Parameter, for NH_3-N, NO_3-N, PO_4^{3-}, COD, SO_4^{2-}, TOC	500 mL	2833249
Wastewater Influent Standard Solution, Mixed Parameter, for NH_3-N, NO_3-N, PO_4, COD, SO_4, TOC	500 mL	2833149

Optional reagents and apparatus

Description	Unit	Item no.
Flask, volumetric, Class A, 100-mL glass	each	1457442
Reactor adapter sleeves, 16 mm to 13 mm diameter, for TNTplus vials	5/pkg	2895805
Sampling bottle with cap, low density polyethylene, 500-mL	12/pkg	2087079
Sulfuric Acid, concentrated, ACS	500 mL	97949
Test tube rack, polyethylene, for 13-mm OD vials, 90 holes	each	2497900
Water, deionized	4 L	27256

HACH

FOR TECHNICAL ASSISTANCE, PRICE INFORMATION AND ORDERING:
In the U.S.A. – Call toll-free 800-227-4224
Outside the U.S.A. – Contact the HACH office or distributor serving you.
On the Worldwide Web – www.hach.com; E-mail – techhelp@hach.com

HACH COMPANY
WORLD HEADQUARTERS
Telephone: (970) 669-3050
FAX: (970) 669-2932

02/2014, Edition 8